Optimal Energy-Efficient Antenna Selection and Power Adaptation for Interference-Outage Constrained Underlay Spectrum Sharing

Suji Naduvilpattu, *Student Member, IEEE*, and Neelesh B. Mehta, *Fellow, IEEE*

***Abstract*— Underlay spectrum sharing addresses spectrum scarcity but imposes constraints on the interference the secondary system causes to the primary receiver. For a secondary transmitter that is subject to the stochastic and general interference-outage constraint and the peak transmit power constraint, we present a novel joint antenna selection and power adaptation rule. It addresses the twin goals of improving the spectral efficiency and reducing the power consumed of an underlay secondary system with low hardware complexity and cost. We prove that the rule maximizes the energy-efficiency (EE) of the secondary system. Its form differs from all other rules considered in the literature. We then present an insightful geometrical characterization of the optimal power of the selected antenna in terms of the channel gains within the secondary system and between the secondary and primary systems. Our approach leads to several special cases, which are themselves novel, and novel analytical insights about the performance and structure of the optimal rule. We also present an iterative subgradient-based algorithm and a simpler non-iterative bound-based algorithm to compute the rule's parameters. The rule achieves a markedly higher EE compared to conventional approaches, and serves as a new fundamental benchmark for antenna selection in underlay spectrum sharing.**

***Index Terms*— Energy-efficiency, spectrum sharing, underlay, antenna selection, power adaptation, interference.**

I. Introduction

NEXT generation wireless systems are required to support much higher data traffic, but under severe constraints on the available spectrum and energy consumed. For example, 5G systems are expected to achieve a three times higher spectral efficiency and a hundred times higher energy-efficiency (EE), while 6G systems are envisaged to achieve a ten times higher spectral efficiency and a hundred times higher EE than their previous generations [2].

Manuscript received 1 December 2021; revised 3 May 2022; accepted 28 June 2022. Date of publication 6 July 2022; date of current version 16 September 2022. This work was supported by a research grant from Intel Corp., Bangalore. An earlier version of this paper was presented in part at the IEEE International Conference on Communications (ICC) 2021 [DOI: 10.1109/ICC42927.2021.9500252]. The associate editor coordinating the review of this article and approving it for publication was L. Song. *(Corresponding author: Suji Naduvilpattu.)*

The authors are with the Department of Electrical Communication Engineering, Indian Institute of Science (IISc), Bengaluru, Bengaluru 560012, India (e-mail: sujivalsala@gmail.com; nbmehta@iisc.ac.in).

Color versions of one or more figures in this article are available at https://doi.org/10.1109/TCOMM.2022.3188836.

Digital Object Identifier 10.1109/TCOMM.2022.3188836

Spectrum sharing is a promising technique that addresses the first goal of improving spectrum utilization and overcoming the critical spectrum shortage. It permits secondary users (SUs) to share the spectrum used by high priority primary users (PUs). In the interweave mode of spectrum sharing, the SU transmits only when the PU is not transmitting. On the other hand, in the underlay mode, both PU and SU transmit simultaneously over the same spectrum, which further improves spectrum utilization [3]. However, the SU is subject to constraints on the interference it causes, in order to protect the PU.

To mitigate the performance degradation of the SU due to the interference constraint imposed in the underlay mode, various multiple antenna techniques have been investigated. Transmit antenna selection (TAS) is one such technique in which the transmitter employs only one radio frequency (RF) chain. It dynamically selects an antenna, connects it to the RF chain, and transmits to the receiver. This is unlike conventional multi-antenna systems, in which the number of RF chains equals the number of antennas. The RF chain contributes the most to the hardware complexity and cost as it consists of several components such as a digital-to-analog converter, mixer, filter, and amplifier. On the other hand, antenna elements are relatively cheap. Thus, TAS exploits spatial diversity, but with a complexity comparable to a single antenna system.

TAS and spectrum sharing have been adopted in practical wireless systems. For example, IEEE 802.11af/be, long term evolution (LTE)-license assisted access, MulteFire, citizen's broadband radio service, and 5G new radio unlicensed employ spectrum sharing. TAS has been adopted in LTE and IEEE 802.11n [4]. TAS for underlay spectrum sharing has also attracted attention in the literature. Symbol error probability-minimizing TAS rules are proposed in [5], [6]. The secondary transmitter (STx) is subject to an interference-outage constraint in [5], and the average interference constraint in [6]. A TAS rule that maximizes the signal-to-interference-plus-noise ratio (SINR) is proposed in [7] for a peak interference power constrained STx. Rate-maximizing TAS is studied in [8] for an STx that is subject to peak interference and transmit power constraints. The above works also differ in the interference constraints they impose on the secondary system. However, EE maximization for underlay spectrum sharing is not considered.

Given the critical importance of EE today, the trade-off between energy consumed and rate also needs to be carefully addressed. EE-maximizing TAS rules are investigated in [9]–[11] for multiple antenna systems, but underlay spectrum sharing is not considered. On the other hand, the EE maximization approaches studied in [12]–[16] for underlay spectrum sharing do not consider TAS. Specifically, power adaptation for EE maximization is studied in [12], [13]. The average interference power constraint and different combinations of peak and average power constraints are considered in [12], while the interference-outage constraint is considered in [13]. In [14], power adaptation is studied for various combinations of peak and average power constraints, and peak and average interference constraints. In [15], power adaptation for a cognitive multiple antenna broadcast channel is studied for the peak power and the peak interference constraints. Power adaptation for the average interference constraint is studied in [16].

A. Contributions

We see that while EE-maximization, TAS, and underlay spectrum sharing have been studied in the literature, a combination of these three topics has not. This combination is relevant given the need to develop practically appealing, low complexity solutions that better utilize the scarce spectrum and transmit as many bits as possible per unit energy by exploiting spatial diversity. The system model, optimization problem, and its solution all change when TAS is considered for maximizing the EE of underlay spectrum sharing. The interference constraint also exerts a crucial influence. We study the stochastic interference-outage constraint, which limits the probability that the interference power at the primary receiver (PRx) exceeds a threshold [5], [17]–[19]. It subsumes the widely-studied and more conservative peak interference constraint, and can lead to higher rates for the secondary system. It is suitable for primary systems that offer delay or disruption-tolerant services that can tolerate outages due to interference. In practical scenarios where the STx has imperfect channel state information (CSI), the STx cannot satisfy the peak interference constraint, but it can satisfy the interference-outage constraint.

We make the following contributions:

- *Optimal Rule:* We propose a novel EE-aware joint antenna selection and power adaptation (EE-ASPA) rule. We prove that it maximizes the EE of a secondary system in which the STx is subject to the interference-outage constraint and the peak power constraint. Given its optimality, EE-ASPA serves as fundamental benchmark for assessing the EE of TAS in underlay spectrum sharing. EE-ASPA jointly selects the antenna and its power to maximize a reward function, whose structure is very different from the rules in [12]–[14], [16]. The function consists of three terms. The first term is the instantaneous rate. The second term is the transmit power weighted by a power penalty η. The third term is an indicator function that checks if the STx-PRx channel power gain exceeds a threshold, and has an interference penalty λ as its weight.
- *Explicit Form of EE-ASPA and Deep Analytical Insights:* An important contribution of our work is an explicit form for the optimal power and an insightful geometric characterization of EE-ASPA. Our analysis also highlights the non-intuitive influence of the interference-outage constraint and the theoretical novelty of the optimal solution. The constraint causes the optimal power to be a discontinuous function of the channel power gain from the STx to the secondary receiver (SRx). Furthermore, the power can remain constant and then jump higher as the STx-SRx channel power gain increases. No such discontinuity arises in the power adaptation considered in [6], [20]–[22]. Such insights do not arise from the numerical optimization techniques used to maximize the EE in [10], [11], [15], [23]–[25].
- *Novel and Insightful Special Cases:* In the small peak power regime, we show that EE-ASPA reduces to a simpler binary power adaptation rule, and the optimal antenna can be selected only on the basis of the STx-SRx channel power gain. We derive the optimal EE and the outage probability in closed-form for this regime. We also present several insightful special cases of EE-ASPA such as the rate-optimal rule and the unconstrained ASPA rule, which are by themselves novel.
- *Determining Penalties Efficiently:* We propose an iterative approach to determine η and prove its convergence to the optimal value. For determining λ, we first propose a subgradient-based iterative algorithm and prove its convergence. We then propose an alternate, computationally simpler non-iterative approach; it uses a tractable upper bound on the outage probability.
- *Benchmarking and Efficacy:* We observe that EE-ASPA increases the EE by up to 200% compared to several conventional rules.

Comments: Table I presents a concise summary of the literature and the many aspects in which it differs from our work. EE-ASPA differs from the EE-maximizing rules in [9]–[11], [24], which depend only on the transmitter-to-receiver channel power gains and not on any interference link gains. Hence, their mathematical form and properties are different. In [12]–[16], [23], [25], EE maximization for underlay spectrum sharing is considered. However, TAS is not considered and the interference constraint is different. As a result, their power adaptation rules differ from EE-ASPA. In [14], the average of the instantaneous EE is maximized. The rules in [15], [23], [25], [26] maximize the instantaneous EE. However, in a system that adapts its power and rate, maximizing the instantaneous EE or the average of the instantaneous EE is not the same as maximizing the EE, which turns out to be the ratio of the average rate to the average energy consumed. In [12], [13], the STx is assumed to know the primary transmitter (PTx)-PRx channel power gain. However, this is practically challenging since the PTx is seldom controlled by the secondary system.

B. Outline and Notations

Section II describes the system model. In Section III, we propose EE-ASPA, prove its optimality, and elucidate its structure. We then present several insights about the optimal rule and its performance. In Section IV, we propose two

TABLE I
COMPARISON OF RELATED LITERATURE ON EE MAXIMIZATION

Reference	*EE metric*	*Underlay spectrum sharing*	*TAS*	*Interference constraint*	*Solution*
Zhou et al. [12]	Average	Yes	No	Average	Closed-form
Jin et al. [26]	Instantaneous	Yes	Yes	Average	Adhoc method based on exhaustive search, bisection
Wang et al. [13]	Average	Yes	No	SINR-outage	Closed-form
Sboui et al. [14]	Average of instantaneous EE	Yes	No	Peak/ Average	Closed-form
Mili et al. [16]	Average	Yes	No	Average	Multi-objective optimization-based adhoc method
Mao et al. [15], Huang et al. [23], Wang et al. [25]	Instantaneous	Yes	No	Peak	Numerical methods
Li et al. [9]	Instantaneous	No	Yes	NA	Closed-form
Zhou et al. [11], Wang et al. [10], Jiang et al. [24]	Instantaneous	No	Yes	NA	Numerical methods

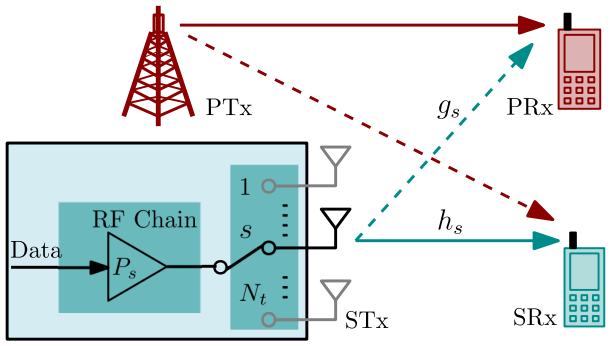

Fig. 1. System model showing the STx with N_t antennas and one RF chain transmitting to the SRx and causing interference at the PRx.

algorithms to determine the constants involved in the rule. Numerical results and our conclusions follow in Sections V and VI, respectively.

Notation: We show scalar variables in normal font, vector variables in lowercase bold font, and sets in calligraphic font. $\Pr(X)$, $\Pr(X \mid Y)$, and $\mathbb{E}[X]$ denote the probability of X, conditional probability of X given Y, and expectation of X, respectively. $f_X(.)$ denotes the probability density function of X. The indicator function is denoted by $\mathbb{1}_{\{a\}}$, which equals one if a is true and is zero else. We denote $\max\{a, 0\}$ as $(a)^+$.

II. SYSTEM MODEL AND PROBLEM FORMULATION

A. System Model

The system model is illustrated in Figure 1. It consists of a primary system and a secondary system that share the same spectrum. The secondary system consists of an STx with N_t transmit antennas and an SRx, which can have one or more antennas. The STx chooses an antenna $s \in \{1, \ldots, N_t\}$ and connects it to the RF chain. It transmits with a power P_s to the SRx. When the SRx has one antenna, let h_s denote the channel power gain from antenna s of the STx to the SRx. In general, when the SRx has N_r antennas, h_s is replaced with $\sum_{j=1}^{N_r} h_{js}$ for maximal ratio combining and $\max_{j\in\{1,\ldots,N_r\}}\{h_{js}\}$ for selection combining, where h_{js} denotes the channel power gain from antenna s of the STx to antenna j of the SRx. Let the channel power gain from antenna s of the STx to the PRx be denoted as g_s. Let $\mathbf{h} \triangleq [h_1, \ldots, h_{N_t}]$ and $\mathbf{g} \triangleq [g_1, \ldots, g_{N_t}]$.

Primary Interference Models: Let α_p denote the baseband channel gain from the PTx to the SRx and P_p denote the primary transmit power. We consider the following two models for the interference from the PTx to the SRx:

- *Instantaneous Interference Power Model [12]–[14], [16]:* In this model, the interference from the PTx is given by $P_p|\alpha_p|^2$, where P_p is the PTx transmit power and α_p is the baseband channel gain from the PTx to the SRx. The SINR Γ at the SRx when the STx transmits from antenna i with power P_i is taken to be $\Gamma = P_i h_i / \left(P_p|\alpha_p|^2 + \sigma_n^2\right)$.
- *Average Interference Power Model [5], [18], [27], [28]:* This model considers the average interference of the PTx-SRx link $\mathbb{E}\left[P_p|\alpha_p|^2\right]$ and writes the SINR as $P_i h_i / \left(\mathbb{E}\left[P_p|\alpha_p|^2\right] + \sigma_n^2\right)$. The model provides a tractable lower bound on the average rate that enables insightful analyses.

CSI Model: The STx knows $\mathbf{h}$ and $\mathbf{g}$ [5], [12], [20]–[22]. In practice, this can be achieved as follows. In the time division duplex mode, the STx can estimate $\mathbf{h}$ and $\mathbf{g}$ using channel reciprocity. In the frequency division duplex mode, the STx can estimate $\mathbf{h}$ via feedback from the SRx, and $\mathbf{g}$ using techniques such as hidden power feedback loop [5]. The SRx performs coherent demodulation. For this, it only needs to know the complex baseband channel gain from the selected STx antenna s to itself, and can estimate it from the pilot symbols transmitted along with the data [21]. Assuming perfect CSI provides an upper limit on the EE with imperfect CSI. The STx also needs to know $P_p|\alpha_p|^2 + \sigma_n^2$ and $\mathbb{E}\left[P_p|\alpha_p|^2\right] + \sigma_n^2$ for the instantaneous and average interference power models, respectively, in order to set its rate. These can be fed back by the SRx.

B. EE-Focused Problem Formulation

The EE of a system, which we denote by EE, is the number of bits transmitted per unit energy consumed. The instantaneous rate in nats/s is $\log(1+\Gamma)$, where $\Gamma = P_s h_s/\sigma^2$ is the SINR. Furthermore, $\sigma^2 = \sigma_p^2 + \sigma_n^2$, where $\sigma_p^2 = P_p|\alpha_p|^2$ for the instantaneous interference power model and $\sigma_p^2 = \mathbb{E}\left[P_p|\alpha_p|^2\right]$ for the average interference power model. The instantaneous power consumed by the STx is $\xi P_s + P_c$, where ξ is the power amplifier inefficiency and P_c is the constant power consumed by components such as mixer, filter, and digital-to-analog converter [12], [29]. For an STx that can adapt its rate and transmit power, it follows from the renewal-reward theorem that

$$\mathsf{EE} = \frac{\mathbb{E}[\log(1+\Gamma)]}{\mathbb{E}[\xi P_s + P_c]}. \quad (1)$$

Thus, EE is the ratio of the average rate to the average power consumed at the STx. The expectations in the numerator and denominator are over both $\mathbf{h}$ and $\mathbf{g}$ for the average interference power model because the transmit power and the selected antenna are a function of both $\mathbf{h}$ and $\mathbf{g}$. For the instantaneous interference power model, the expectations are over $\mathbf{h}$, $\mathbf{g}$, and σ_p^2.

Constraints: The secondary system is subject to the following constraints:

1) *Interference-Outage Constraint:* An interference-outage occurs at the PRx when the interference power $P_s g_s$ exceeds a threshold τ. The constraint requires that an interference-outage can occur with a probability at most $O_{\max}$, i.e., $\Pr(P_s g_s > \tau) \leq O_{\max}$. The peak interference constraint is a special case of this and corresponds to $O_{\max} = 0$.
2) *Peak Power Constraint:* The transmit power P_s must not exceed the peak power $P_{\max}$ [12].

Comments: The average of the instantaneous EE, which is used in [14], is not the same as EE because the expectation of a ratio is not the same as a ratio of expectations. We note that maximizing the instantaneous EE is not meaningful for a secondary subject to a stochastic interference constraint, since the actions of the ASPA rule over the entire space of realizations of the channel gains determine whether it satisfies the constraint.

An ASPA rule ϕ specifies, for *each realization* of the channel power gains, the transmit antenna $s \in \{1, \ldots, N_t\}$ and its transmit power $P_s \in [0, P_{\max}]$. Let $\mathcal{D}$ be the set of all ASPA rules. For the average interference power model, the problem $\mathcal{P}_0$ for finding an optimal ASPA rule can be stated as the following constrained stochastic optimization problem:

$$\mathcal{P}_0: \quad \max_{\phi \in \mathcal{D}} \quad \left\{ \frac{\mathbb{E}\left[\log\left(1 + \frac{P_s h_s}{\sigma^2}\right)\right]}{\mathbb{E}\left[\xi P_s + P_c\right]} \right\}, \tag{2}$$

$$\text{s.t.} \quad \Pr(P_s g_s > \tau) \leq O_{\max}, \tag{3}$$

$$0 \leq P_s \leq P_{\max}, \tag{4}$$

$$(s, P_s) = \phi(\mathbf{h}, \mathbf{g}). \tag{5}$$

Here, $\phi : (\mathbb{R}^+)^{N_t} \times (\mathbb{R}^+)^{N_t} \rightarrow \{1, \ldots, N_t\} \times [0, P_{\max}]$; it takes $\mathbf{h}$ and $\mathbf{g}$ as inputs and outputs s and P_s. For the instantaneous interference power model, ϕ is a mapping from $(\mathbb{R}^+)^{N_t} \times (\mathbb{R}^+)^{N_t} \times \mathbb{R}^+$ to $\{1, \ldots, N_t\} \times [0, P_{\max}]$ since its inputs are $\mathbf{h}$, $\mathbf{g}$, and σ_p^2. The dependence on σ_p^2 is not shown.

The above formulation can be generalized to include a minimum rate constraint for the STx. We discuss it below.

III. EE-ASPA and Its Optimality

First, we present the EE-maximizing ASPA for the *unconstrained regime*, in which the interference-outage constraint is inactive. Then, we present the general EE-ASPA rule and prove its optimality. Lastly, we present several insights about the structure and performance of EE-ASPA. We shall say that a solution is feasible when it satisfies the interference-outage and peak power constraints. EE-ASPA and the proof of its optimality apply to both interference models. Unless mentioned otherwise, we consider the average interference power model below.

A. Unconstrained Regime

When the constraint in (3) is inactive, we can show that the optimal rule is given by

$$s = \underset{i \in \{1, \ldots, N_t\}}{\operatorname{argmax}} \{h_i\} \text{ and } P_s = \min\left\{\widetilde{P}(h_s), P_{\max}\right\}, \tag{6}$$

where $\widetilde{P}(h_s) = \left(1/\eta\xi - \sigma^2/h_s\right)^+$ and $\eta \geq 0$ is a constant. Its proof is a simpler version of the proof in Section III-B and is not shown here to conserve space. We shall refer to this rule as the *unconstrained ASPA (UC-ASPA)* rule. In this regime, the optimal rule is independent of the STx-PRx link gains, and the antenna with the largest STx-SRx channel power gain is selected.

B. Constrained Regime

Consider the following rule, which we shall refer to as EE-ASPA:

$$(s^*, P_{s^*}^*) \stackrel{\triangle}{=} \underset{P_i \in [0, P_{\max}],\ i \in \{1, \ldots, N_t\}}{\operatorname{argmax}} \{\Omega_i(P_i; \eta, \lambda)\}, \tag{7}$$

where s^* is the selected antenna, $P_{s^*}^*$ is its transmit power, and

$$\Omega_i(P_i; \eta, \lambda) \stackrel{\triangle}{=} \log\left(1 + \frac{P_i h_i}{\sigma^2}\right) - \eta\xi P_i - \lambda \mathbb{1}_{\{P_i g_i > \tau\}}, \tag{8}$$

is the reward function. Here, $\eta \geq 0$ and $\lambda \geq 0$ are two constants. To keep the notation simple, we do not explicitly show the dependence of $\Omega_i(P_i; \eta, \lambda)$ on the channel power gains.

The following lemmas prove that the above form of EE-ASPA solves $\mathcal{P}_0$. Lemma 1 proves that EE-ASPA maximizes an optimization problem $\mathcal{P}_1(\eta)$ with a transformed objective function that is parameterized by η. Lemma 2 shows that the value of η at which the objective function of $\mathcal{P}_1(\eta)$ achieves the maximum value of 0 is the optimal EE and that EE-ASPA achieves it. Lemma 3 proves the convergence of an iterative algorithm to the optimal η.

Lemma 1: For a given $\eta \geq 0$, let λ be chosen such that $\Pr(P_{s^*}^* g_{s^*} > \tau) = O_{\max}$, where $(s^*, P_{s^*}^*) = \phi^*(\mathbf{h}, \mathbf{g})$ and ϕ^* is defined in (7). Then, ϕ^* solves the following problem:

$$\mathcal{P}_1(\eta): \quad \max_{\phi \in \mathcal{D}} \quad \left\{ \mathbb{E}\left[\log\left(1 + \frac{P_s h_s}{\sigma^2}\right)\right] - \eta \mathbb{E}\left[\xi P_s + P_c\right] \right\},$$
$$\text{s.t.} \quad (3),\ (4),\ (5). \tag{9}$$

Proof: The proof is given in Appendix A. ∎

Lemma 2: Let η^* be the power penalty at which the maximum value of the objective function of $\mathcal{P}_1(\eta)$ is 0. For this value of η^*, let λ^* be chosen such that $\Pr(P_{s^*}^* g_{s^*} > \tau) = O_{\max}$, where $(s^*, P_{s^*}^*) = \phi^*(\mathbf{h}, \mathbf{g})$. Then, η^* is the optimal EE of $\mathcal{P}_0$ and ϕ^* solves $\mathcal{P}_0$.

Proof: The proof is given in Appendix B. ∎

Lemmas 1 and 2 imply that ϕ^* is the EE-optimal ASPA rule. However, Lemma 2 requires the optimal EE η^* to be specified. It can be determined iteratively as follows. In the u^{th} iteration, given $\eta = \eta^{(u)}$, let $\lambda^{(u)}$ denote the corresponding interference penalty at which $\Pr(P_{s^{(u)}} g_{s^{(u)}} > \tau) = O_{\max}$. Here, $s^{(u)}$ is the optimal antenna and $P_{s^{(u)}}$ is its optimal power in the u^{th}

iteration; both are functions of the channel power gains and are determined from (7). Then, consider the following update rule:

$$\eta^{(u+1)} = \frac{\mathbb{E}\left[\log\left(1+\frac{P_{s^{(u)}}h_{s^{(u)}}}{\sigma^2}\right)\right]}{\mathbb{E}\left[\xi P_{s^{(u)}}+P_c\right]}, \tag{10}$$

with $\eta^{(0)}=0$. The algorithm terminates when the objective function of $\mathcal{P}_1(\eta)$ is close to 0.

Lemma 3: The sequence $\eta^{(0)},\eta^{(1)},\ldots$ is monotonically increasing and converges to η^*.

Proof: The proof is given in Appendix C. ∎

Note that η and λ are functions of the system parameters τ, $O_{\max}$, $P_{\max}$, ξ, P_c, and N_t. We now present a key result of the paper, which is an explicit characterization of the optimal transmit power and antenna.

Result 1: The optimal antenna s^* is given by

$$s^* = \underset{i\in\{1,\ldots,N_t\}}{\text{argmax}} \left\{\Omega_i\left(P_i^*;\eta^*,\lambda^*\right)\right\}, \tag{11}$$

where P_i^* is the optimal power if antenna i is selected. The optimal power depends on which among four regions (h_i,g_i) lies in. The regions $\mathcal{R}_1,\mathcal{R}_2,\mathcal{R}_3$, and $\mathcal{R}_4$ are defined as follows:

$$\mathcal{R}_1 = \left\{(h_i,g_i): g_i \le \frac{\tau}{P_{\max}}\right\}, \tag{12a}$$

$$\mathcal{R}_2 = \left\{(h_i,g_i): h_i \le \alpha_1(g_i),\ g_i > \frac{\tau}{P_{\max}}\right\}, \tag{12b}$$

$$\mathcal{R}_3 = \left\{(h_i,g_i): \alpha_1(g_i) < h_i \le \alpha_2,\ g_i > \frac{\tau}{P_{\max}}\right\}, \tag{12c}$$

$$\mathcal{R}_4 = \left\{(h_i,g_i): h_i > \alpha_2,\ g_i > \frac{\tau}{P_{\max}}\right\}, \tag{12d}$$

where

$$\alpha_0 = \eta^*\xi\sigma^2,\ \alpha_1(g_i) = \frac{\alpha_0}{\left(1-\frac{\eta^*\xi\tau}{g_i}\right)^+},\ \text{and}$$

$$\alpha_2 = \frac{\alpha_0}{\left(1-\eta^*\xi P_{\max}\right)^+}. \tag{13}$$

The optimal transmit power is given by

$$P_i^* = \begin{cases} \min\left\{\widetilde{P}\left(h_i\right), P_{\max}\right\}, & \text{if } (h_i,g_i)\in\mathcal{R}_1, \quad (14a)\\ \widetilde{P}\left(h_i\right), & \text{if } (h_i,g_i)\in\mathcal{R}_2, \quad (14b)\\ \underset{P_i\in\left\{\widetilde{P}(h_i),\tau/g_i\right\}}{\text{argmax}} \left\{\Omega_i\left(P_i;\eta^*,\lambda^*\right)\right\}, & \text{if } (h_i,g_i)\in\mathcal{R}_3, \quad (14c)\\ \underset{P_i\in\{P_{\max},\tau/g_i\}}{\text{argmax}} \left\{\Omega_i\left(P_i;\eta^*,\lambda^*\right)\right\}, & \text{if } (h_i,g_i)\in\mathcal{R}_4, \quad (14d)\end{cases}$$

where

$$\widetilde{P}\left(h_i\right) = \sigma^2\left(\frac{1}{\alpha_0}-\frac{1}{h_i}\right)^+. \tag{15}$$

Proof: The proof is given in Appendix D. ∎

Note that (14c) and (14d) require comparing the reward function at only two power values. The decision regions and the corresponding optimal power are illustrated for EE-ASPA and UC-ASPA in Figures 2(a) and 2(b), respectively.

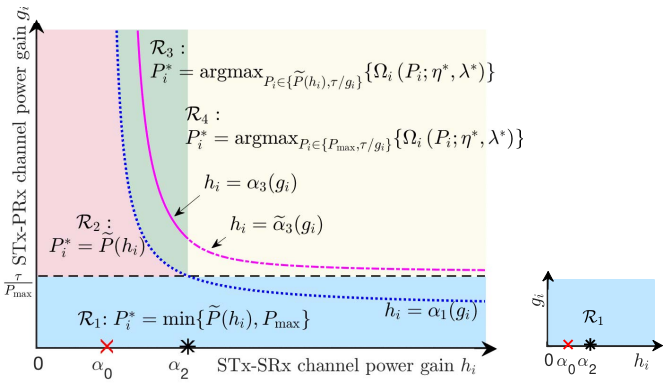

(a) EE-ASPA (b) UC-ASPA

Fig. 2. Decision regions that govern how the optimal transmit power P_i^* depends on h_i and g_i.

Understanding the Geometric Representation: We say that antenna i is *non-outage-inducing* if $P_i^* g_i \le \tau$, else it is *outage-inducing*. Result 1 provides deep insights into when an antenna is outage-inducing and when it is not, and what its transmit power will be in each case. Consider first UC-ASPA. It has only one decision region. In it, the antenna is non-outage-inducing even if it transmits with the maximum power $P_{\max}$.

In general, for EE-ASPA five key values of h_i, namely, α_0, $\alpha_1(g_i)$, α_2, $\alpha_3(g_i)$, and $\widetilde{\alpha}_3(g_i)$ define the four regions. α_0, $\alpha_1(g_i)$, and α_2 are the values of h_i at which $\widetilde{P}\left(h_i\right)$ in (15) first becomes non-zero, becomes equal to τ/g_i, and becomes equal to $P_{\max}$, respectively. Their expressions in Result 1 can be derived easily using (15). $\alpha_3(g_i)$ and $\widetilde{\alpha}_3(g_i)$ are the values of h_i at which $\Omega_i\left(\tau/g_i;\eta^*,\lambda^*\right)$ becomes equal to $\Omega_i\left(\widetilde{P}\left(h_i\right);\eta^*,\lambda^*\right)$ and $\Omega_i\left(P_{\max};\eta^*,\lambda^*\right)$, respectively. We derive their expressions below.

a) Region $\mathcal{R}_1$: From the definition of α_0 and (14a), we get $P_i^*=0$ for $h_i\le\alpha_0$. Since $\widetilde{P}\left(h_i\right)>P_{\max}$ for $h_i>\alpha_2$, we get $P_i^*=P_{\max}$ for $h_i>\alpha_2$. From (12a), it follows that antenna i is non-outage-inducing in all of $\mathcal{R}_1$.

b) Region $\mathcal{R}_2$: We can verify from (15) and the expression for P_i^* in (14b) that $P_i^*=\widetilde{P}\left(h_i\right)\le\tau/g_i$ for $h_i\le\alpha_1(g_i)$. Hence, the antenna is non-outage-inducing in all of $\mathcal{R}_2$.

c) Region $\mathcal{R}_3$: Equating $\Omega_i\left(\tau/g_i;\eta^*,\lambda^*\right)$ and $\Omega_i\left(\widetilde{P}\left(h_i\right);\eta^*,\lambda^*\right)$ at $h_i=\alpha_3(g_i)$, we can show that

$$\alpha_3(g_i) = \frac{\alpha_0}{\left(\omega_{\lambda^*}-\frac{\eta^*\xi\tau}{g_i}\right)^+}, \tag{16}$$

where $\omega_{\lambda^*} = -W_0\left(-e^{-1-\lambda^*}\right)$ and $W_0(.)$ denotes the LambertW function on its principal branch [30]. Also, we have $\Omega_i\left(\tau/g_i;\eta^*,\lambda^*\right)\ge\Omega_i\left(\widetilde{P}\left(h_i\right);\eta^*,\lambda^*\right)$ for $h_i\in(\alpha_1(g_i),\alpha_3(g_i)]$ and $\Omega_i\left(\tau/g_i;\eta^*,\lambda^*\right)<\Omega_i\left(\widetilde{P}\left(h_i\right);\eta^*,\lambda^*\right)$ for $h_i\in(\alpha_3(g_i),\alpha_2]$. Thus, $P_i^*=\tau/g_i$ when $\alpha_1(g_i)<h_i\le\alpha_3(g_i)$, and is $\widetilde{P}\left(h_i\right)$ otherwise. Since $\tau/g_i<\widetilde{P}\left(h_i\right)\le P_{\max}$ in $\mathcal{R}_3$, antenna i is outage-inducing only when $h_i\in(\alpha_3(g_i),\alpha_2]$. When $\alpha_3(g_i)>\alpha_2$, $P_i^*=\tau/g_i$ and the antenna is non-outage-inducing in all of $\mathcal{R}_3$.

d) Region $\mathcal{R}_4$: Equating $\Omega_i\left(\tau/g_i;\eta^*,\lambda^*\right)$ and $\Omega_i\left(P_{\max};\eta^*,\lambda^*\right)$ at $h_i=\widetilde{\alpha}_3(g_i)$, we can show that

$$\widetilde{\alpha}_3(g_i)=\frac{\sigma^2-\sigma^2 e^{-\lambda^*+\eta^*\xi\left(\frac{\tau}{g_i}-P_{\max}\right)}}{\left(e^{-\lambda^*+\eta^*\xi\left(\frac{\tau}{g_i}-P_{\max}\right)}P_{\max}-\frac{\tau}{g_i}\right)^+}. \tag{17}$$

Also, we get $\Omega_i\left(\tau/g_i;\eta^*,\lambda^*\right)\geq\Omega_i\left(P_{\max};\eta^*,\lambda^*\right)$ for $h_i\in(\alpha_2,\widetilde{\alpha}_3(g_i)]$ and $\Omega_i\left(\tau/g_i;\eta^*,\lambda^*\right)<\Omega_i\left(P_{\max};\eta^*,\lambda^*\right)$ for $h_i>\widetilde{\alpha}_3(g_i)$. Thus, $P_i^*=\tau/g_i$ for $h_i\in(\alpha_2,\widetilde{\alpha}_3(g_i)]$, and $P_i^*=P_{\max}$ for $h_i>\widetilde{\alpha}_3(g_i)$. Since $\tau/g_i<P_{\max}<\widetilde{P}\left(h_i\right)$, in $\mathcal{R}_4$, antenna i is outage-inducing only if $h_i>\widetilde{\alpha}_3(g_i)$.

1) Significance of η and λ: The power penalty η controls the power consumption. For example, from Result 1, α_0 increases as η increases, i.e., the region where the optimal power is 0 enlarges and the transmit power P_i^* decreases. λ determines when an interference-outage occurs. As λ increases, the interference-outage constraint becomes tighter and EE-ASPA rule selects a non-outage-inducing power more often. Setting $\lambda=0$ yields the UC-ASPA rule.

Setting $\eta=0$ results in the following rule, which can be shown to maximize the average rate. To the best of our knowledge, even this special case is not available in the literature.

Corollary 1: The optimal ASPA rule that maximizes the average rate subject to the interference-outage and peak power constraints is as follows:

$$P_i=\begin{cases}\frac{\tau}{g_i}, & \text{if } P_{\max}\in\left[\frac{\tau}{g_i},\frac{\sigma^2}{h_i}e^{\lambda}\left(1+\frac{\tau h_i}{\sigma^2 g_i}\right)-\frac{\sigma^2}{h_i}\right),\\ P_{\max}, & \text{else,}\end{cases} \tag{18a}$$

$$s=\underset{i\in\{1,\ldots,N_t\}}{\operatorname{argmax}}\left\{\log\left(1+\frac{P_i h_i}{\sigma^2}\right)-\lambda\mathbb{1}_{\{P_i g_i>\tau\}}\right\}, \tag{18b}$$

where λ is chosen such that $\Pr\left(P_s g_s>\tau\right)=O_{\max}$.

C. Additional Minimum Rate Constraint

Now, the STx is subject to the additional constraint: $\mathbb{E}\left[\log\left(1+\frac{P_s h_s}{\sigma^2}\right)\right]\geq R_{\min}$, where $R_{\min}$ is the minimum rate. Then, the optimal rule can be shown to be

$$(s,P_s)\triangleq\underset{P_i\in[0,P_{\max}],\ i\in\{1,\ldots,N_t\}}{\operatorname{argmax}}\left\{(1+\delta)\log\left(1+\frac{P_i h_i}{\sigma^2}\right)-\eta\xi P_i-\lambda\mathbb{1}_{\{P_i g_i>\tau\}}\right\}, \tag{19}$$

where $\delta\geq 0$ is chosen to satisfy the above average rate constraint with equality, and η and λ are defined as before. For this rule, the transmit power again depends on which of the four regions (h_i,g_i) lies in. However, the parameters that define the regions' boundaries change to: $\alpha_0(\delta)=\eta\xi\sigma^2/(\delta+1)$, $\alpha_2(\delta)=\alpha_0(\delta)/(1-\eta\xi P_{\max}/(1+\delta))^+$, $\alpha_1(g_i,\delta)=\alpha_0(\delta)/\left(1-\frac{\eta\xi\tau}{g_i(1+\delta)}\right)^+$, $\alpha_3(g_i,\delta)=\alpha_0(\delta)/\left(\omega-\frac{\eta\xi\tau}{g_i(1+\delta)}\right)^+$, and $\widetilde{\alpha}_3(g_i,\delta)=\frac{\sigma^2-\sigma^2 e^{-\frac{\lambda}{\delta+1}+\frac{\eta\xi}{\delta+1}\left(\frac{\tau}{g_i}-P_{\max}\right)}}{\left(e^{-\frac{\lambda}{\delta+1}+\frac{\eta\xi}{\delta+1}\left(\frac{\tau}{g_i}-P_{\max}\right)}P_{\max}-\frac{\tau}{g_i}\right)^+}$, where $\omega=-\mathcal{W}_0\left(-e^{-1-\frac{\lambda}{1+\delta}}\right)$.

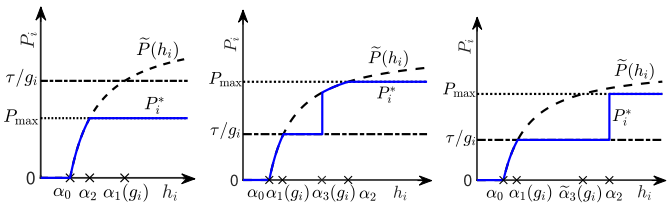

(a) For $P_{\max}\leq\frac{\tau}{g_i}$ (b) For $P_{\max}>\frac{\tau}{g_i}$ and $\alpha_3(g_i)\leq\alpha_2$ (c) For $P_{\max}>\frac{\tau}{g_i}$ and $\alpha_3(g_i)>\alpha_2$

Fig. 3. Non-decreasing and discontinuous behavior of P_i^* as a function of h_i for a given g_i for three scenarios.

D. Structural Insight: Non-Decreasing and Discontinuous Behavior of P_i^*

The following corollary shows two rather non-intuitive aspects about the optimal power that arise due to the interference-outage constraint. First, the optimal power P_i^* can be a discontinuous function of the STx-SRx channel power gain h_i. Second, the transmit power can remain constant at τ/g_i even when h_i increases. This is because the interference-outage constraint penalizes the STx if the interference power exceeds the threshold τ.

Corollary 2: The P_i^* is a monotonically non-decreasing, but possibly discontinuous, function of the STx-SRx channel power gain h_i for a given STx-PRx channel power gain g_i. The discontinuity can occur at no more than one point, which is either $\alpha_3(g_i)$ or $\widetilde{\alpha}_3(g_i)$.

Proof: The proof is given in Appendix E. ∎

The result is illustrated in Figure 3 for three scenarios. Figure 3(a) arises when $P_{\max}\leq\tau/g_i$, which corresponds to $\mathcal{R}_1$. There is no discontinuity in P_i^* for this scenario because $\mathcal{R}_1$ is a non-outage-inducing region. Figures 3(b) and 3(c) correspond to $P_{\max}>\tau/g_i$ and discontinuities occur at $\alpha_3(g_i)$ and $\widetilde{\alpha}_3(g_i)$, respectively, in them. Such insights are hard to obtain from the numerical optimization-based approaches pursued in the literature [15], [23], [25].

E. Insight: Reduction to Binary Power Adaptation in Small $P_{\max}$ Regime

Next, we consider the small $P_{\max}$ regime. Since the transmit power is small, the interference-outage constraint is inactive and $P_s\ll P_c$. Hence, the objective function in $\mathcal{P}_0$ reduces to $\mathbb{E}\left[\log\left(1+P_s h_s/\sigma^2\right)\right]/P_c$. It is maximized when the antenna with the largest STx-SRx channel power gain is selected: $s^*=\underset{i\in\{1,\ldots,N_t\}}{\operatorname{argmax}}\{h_i\}$. Furthermore, from the expressions for α_0 and α_2 in (13), it follows that $\alpha_2\to\alpha_0$ as $P_{\max}\to 0$. Hence, the regions $\mathcal{R}_2$, $\mathcal{R}_3$, and $\mathcal{R}_4$ shrink and eventually disappear as $P_{\max}$ decreases. From (14a), we get

$$P_i^*=\begin{cases}0, & \text{if } h_i\leq\alpha_0,\\ P_{\max}, & \text{else.}\end{cases} \tag{20}$$

For this simpler rule, the interference-outage probability $P_{\text{out}}=\Pr\left(P_{s^*}^* g_{s^*}>\tau\right)$ and the optimal EE η^* are given as follows for the average interference power model and when the SRx is equipped with a single antenna. $h_1,\ldots,h_{N_t}$ are independent and identically distributed (i.i.d.) exponential

random variables with unit power, and so are $g_1, \ldots, g_{N_t}$ [7], [20]–[22]; this corresponds to Rayleigh fading.

Result 2: In the small $P_{\max}$ regime, P_{out} is given in closed-form by

$$P_{\text{out}} = N_t e^{-\frac{\tau}{P_{\max}}} \sum_{m=0}^{N_t-1} \binom{N_t-1}{m} \frac{(-1)^m}{m+1} e^{-(m+1)\alpha_0}. \quad (21)$$

η^* is the unique fixed-point solution of the following equation:

$$\eta = N_t \left[\xi P_{\max} \left(1 - \left[1 - e^{-\eta\xi\sigma^2} \right]^{N_t} \right) + P_c \right]^{-1} \times \sum_{m=0}^{N_t-1} \binom{N_t-1}{m} \frac{(-1)^m}{m+1} \left[\log\left(1+\eta\xi P_{\max}\right) e^{-(m+1)\eta\xi\sigma^2} + e^{\frac{(m+1)\sigma^2}{P_{\max}}} E_1\left(\frac{(m+1)\sigma^2}{P_{\max}} + \eta\xi(m+1)\sigma^2 \right) \right], \quad (22)$$

where $E_1(x) = \int_x^\infty \frac{e^{-t}}{t} dt$ is the exponential integral [31, Ch. 5.1].

Proof: The proof is given in Appendix F. ∎

We see that, $P_{\text{out}} \propto e^{-\frac{\tau}{P_{\max}}}$ increases as $P_{\max}$ increases. However, its rate of increase, which is proportional to $e^{-\frac{\tau}{P_{\max}}}/P_{\max}^2$, decreases. Equation (22) brings out how η^* is influenced by $P_{\max}$, P_c, ξ, and N_t. Using (22), η^* can be found using a simple one-dimensional numerical search.

F. Insight: Behavior of EE-ASPA in Large $P_{\max}$ Regime

As $P_{\max}$ increases, from (12), we can see that the regions $\mathcal{R}_1$ and $\mathcal{R}_4$ shrink and disappear. Thus, for large $P_{\max}$, only regions $\mathcal{R}_2$ and $\mathcal{R}_3$ matter. They can be divided into the following four subregions based on the value of P_i^*. In $\mathcal{R}_2$, the subregion $\mathcal{R}_2^{\text{ZP}}$ corresponds to $P_i^* = 0$ (zero power) and the subregion $\mathcal{R}_2^{\text{NOI}}$ corresponds to $P_i^* = \widetilde{P}(h_i) > 0$ (non-outage-inducing). Similarly, the subregion $\mathcal{R}_3^{\text{TP}}$ corresponds to $P_i^* = \tau/g_i$ (threshold power) and the subregion $\mathcal{R}_3^{\text{OI}}$ corresponds to $P_i^* = \widetilde{P}(h_i)$ (outage-inducing). They are given as follows:

$$\begin{aligned}
\mathcal{R}_2^{\text{ZP}} &= \{(h_i, g_i) : h_i \le \alpha_0\}, \text{ where } P_i^* = 0, \\
\mathcal{R}_2^{\text{NOI}} &= \{(h_i, g_i) : \alpha_0 < h_i \le \alpha_1(g_i)\}, \text{ where } P_i^* = \widetilde{P}(h_i), \\
\mathcal{R}_3^{\text{TP}} &= \{(h_i, g_i) : \alpha_1(g_i) < h_i \le \alpha_3(g_i)\}, \text{ where } P_i^* = \frac{\tau}{g_i}, \\
\mathcal{R}_3^{\text{OI}} &= \{(h_i, g_i) : h_i > \alpha_3(g_i)\}, \text{ where } P_i^* = \widetilde{P}(h_i) > \frac{\tau}{g_i}.
\end{aligned} \quad (23)$$

Thus, an antenna induces an interference-outage only when it falls in $\mathcal{R}_3^{\text{OI}}$.

IV. Determining Penalty Constants and a Novel Bound-Based Algorithm

We now present two algorithms to determine η and λ. Both algorithms update η as per the iteration in (10). For a given η, the first algorithm finds the corresponding λ iteratively, while the second one uses a tractable bound on P_{out} to find λ directly and with lower complexity.

A. Subgradient-Based Iterative Algorithm

Let $\lambda^{(\ell-1)}$ denote the value of λ in the $(\ell-1)^{\text{th}}$ iteration. Then, in the ℓ^{th} iteration, the outage probability $P_{\text{out}}^{(\ell)}$, for which no closed-form expression is available, is determined numerically using the Monte Carlo method. Specifically, for N_{fade} realizations of $\mathbf{h}$ and $\mathbf{g}$, the optimal antenna and power are determined for each of them as per (11) and (14).[1] $P_{\text{out}}^{(\ell)}$ is then the fraction of realizations in which $P_i g_i > \tau$. The variance of the error due to the Monte Carlo method decreases as $\mathcal{O}(1/N_{\text{fade}})$. Then, λ is updated as

$$\lambda^{(\ell)} = \left[\lambda^{(\ell-1)} - t \left(O_{\max} - P_{\text{out}}^{(\ell)} \right) \right]^+, \quad (24)$$

where t is the step size. The algorithm terminates when either $P_{\text{out}}^{(\ell)} = O_{\max}$ or $\lambda^{(\ell)} = 0$. We refer to this approach, in which η is updated as per (10) and the corresponding λ is obtained by the subgradient algorithm, as the *subgradient-based algorithm*.

Convergence and Computational Complexity: For a given η and a large N_{fade}, the subgradient algorithm is guaranteed to converge to the neighborhood of the value of λ that satisfies the interference-outage constraint with equality when a constant step size is used. This follows from [32, Prop. 3.2.3] because in the ℓ^{th} iteration, the subgradient $O_{\max} - P_{\text{out}}^{(\ell)}$ is upper bounded by $O_{\max}$, for any ℓ. If the subgradient-based algorithm takes N_{itr} iterations to converge to η^* and N_{sub} iterations to find λ given η, and uses N_{fade} channel realizations in its Monte Carlo computation, its computational complexity is $\mathcal{O}\left(N_{\text{itr}} N_{\text{sub}} N_{\text{fade}}\right)$. This is the same as that of the algorithms in [12], [13], whereas it is $\mathcal{O}\left(N_{\text{sub}} N_{\text{fade}}\right)$ in [16].

B. Bound-Based Non-Iterative Algorithm

We now propose a non-iterative method to find λ. It requires $\mathcal{O}\left(N_{\text{itr}} N_{\text{fade}}\right)$ computations, which is less than that the subgradient method. Given η, we compute the corresponding λ by solving the equation $P_{\text{out}}^{\text{UB}}(\lambda) = O_{\max}$, where $P_{\text{out}}^{\text{UB}}(\lambda)$ is an upper bound on P_{out} that we derive below for the average interference power model.[2] Since $P_{\text{out}} \le P_{\text{out}}^{\text{UB}}(\lambda)$, the solution obtained is feasible.

Given the involved form of EE-ASPA, we focus on the large $P_{\max}$ regime and one receive antenna at the SRx to derive $P_{\text{out}}^{\text{UB}}(\lambda)$. In the next section, we numerically assess the efficacy of this approach for smaller $P_{\max}$ as well. We first show that P_{out} can be written as follows.

Lemma 4: In the large $P_{\max}$ regime, the expression for P_{out} can be written as

$$P_{\text{out}} = N_t \mathbb{E}\left[\left(T_0(h_1) + T_1(h_1) + T_2(h_1) + T_3(h_1) \right)^{N_t-1} \times \Pr\left(h_1 > \alpha_3(g_1) \mid h_1 \right) \right], \quad (25)$$

where

$$T_0(h_1) = \Pr\left(h_2 \le \alpha_0, \Omega_1\left(\widetilde{P}(h_1); \eta^*, \lambda^* \right) > 0 \mid h_1 \right), \quad (26)$$

[1] For the instantaneous interference power model, N_{fade} realizations of $\mathbf{h}$, $\mathbf{g}$, and σ_p^2 are considered.

[2] We note that the analysis for the instantaneous interference power model is intractable because σ_p^2 needs to be averaged over.

$$T_1(h_1) = \Pr\Big(\alpha_0 < h_2 \le \alpha_1(g_2), \Omega_1\left(\widetilde{P}\left(h_1\right); \eta^*, \lambda^*\right) > \Omega_2\left(\widetilde{P}\left(h_2\right); \eta^*, \lambda^*\right) \mid h_1\Big), \quad (27)$$

$$T_2(h_1) = \Pr\Big(\alpha_1(g_2) < h_2 \le \alpha_3(g_2), \Omega_1\left(\widetilde{P}\left(h_1\right); \eta^*, \lambda^*\right) > \Omega_2\left(\frac{\tau}{g_2}; \eta^*, \lambda^*\right) \mid h_1\Big), \quad (28)$$

$$T_3(h_1) = \Pr\Big(h_2 > \alpha_3(g_2), \Omega_1\left(\widetilde{P}\left(h_1\right); \eta^*, \lambda^*\right) > \Omega_2\left(\widetilde{P}\left(h_2\right); \eta^*, \lambda^*\right) \mid h_1\Big). \quad (29)$$

Proof: The proof is given in Appendix G. ∎

$T_0(h_1), T_1(h_1), T_2(h_1)$, and $T_3(h_1)$ are the joint conditional probabilities that, given h_1, antenna 1 is chosen over antenna 2 and antenna 2 lies in the subregions $\mathcal{R}_2^{\text{ZP}}$, $\mathcal{R}_2^{\text{NOI}}$, $\mathcal{R}_3^{\text{TP}}$, and $\mathcal{R}_3^{\text{OI}}$, respectively. Using Lemma 4, we now derive an expression for $P_{\text{out}}^{\text{UB}}(\lambda)$ when the SRx and PRx have one antenna each and the channels undergo i.i.d. Rayleigh fading.

Result 3: In the large $P_{\max}$ regime and Rayleigh fading, $P_{\text{out}}^{\text{UB}}(\lambda)$ is given as

$$P_{\text{out}}^{\text{UB}}(\lambda) = N_t \mathbb{E}\left[e^{-\eta^*\xi\tau/\left(\omega_{\lambda^*} - \frac{\alpha_0}{h_1}\right)} \mathbb{1}_{\left\{h_1 > \frac{\alpha_0}{\omega_{\lambda^*}}\right\}} \times \left[T_0(h_1) + T_1^{\text{UB}}(h_1) + T_2^{\text{UB}}(h_1) + T_3^{\text{UB}}(h_1)\right]^{N_t-1}\right]. \quad (30)$$

The four terms $T_0(h_1)$, $T_1^{\text{UB}}(h_1)$, $T_2^{\text{UB}}(h_1)$, and $T_3^{\text{UB}}(h_1)$ are given as follows:

$$T_0(h_1) = \left(1 - e^{-\alpha_0}\right) \mathbb{1}_{\left\{\psi(h_1) > \alpha_0 e^{1+\lambda^*}\right\}}, \quad (31)$$

where $\psi(h_1) = h_1 e^{\frac{\alpha_0}{h_1}}$.

$$T_1^{\text{UB}}(h_1) = \left[e^{-\alpha_0} - e^{\alpha_0 - \psi(h_1)e^{-\lambda^*}}\left(1 - e^{-\beta_1(h_1)}\right) - e^{-\frac{\alpha_0\beta_1(h_1)}{\beta_1(h_1) - \eta^*\xi\tau} - \beta_1(h_1)}\right] \mathbb{1}_{\left\{\psi(h_1)e^{-\lambda^*} > 2\alpha_0\right\}}, \quad (32)$$

where $\beta_1(h_1) = \eta^*\xi\tau/\left(1 - \alpha_0/\left[\psi(h_1)e^{-\lambda^*} - \alpha_0\right]\right)$.

$$\begin{aligned} T_2^{\text{UB}}(h_1) &= \Bigg[e^{-\beta_2(h_1)-\alpha_0} - e^{-\frac{\alpha_0\beta_2(h_1)}{\omega_{\lambda^*}(\beta_2(h_1) - \eta^*\xi\tau)} - \frac{\beta_2(h_1)}{\omega_{\lambda^*}}} \\ &\quad - \alpha_0\eta^*\xi\tau\, e^{\eta^*\xi\tau(\alpha_0-1)-\alpha_0} E_1\left(\beta_2(h_1) + \eta^*\xi\tau(\alpha_0 - 1)\right) \\ &\quad - \left[\gamma(h_1) + 1\right]^{-1}\left(e^{-\beta_2(h_1)[\gamma(h_1)+1]} - e^{-\frac{\beta_2(h_1)}{\omega_{\lambda^*}}[\gamma(h_1)+1]}\right)\Bigg] \\ &\quad \times \mathbb{1}_{\left\{\psi(h_1) > \alpha_0 e^{\lambda^*}\right\}}, \end{aligned} \quad (33)$$

where $\gamma(h_1) = \frac{\sigma^2}{\tau}\left(\frac{\psi(h_1)e^{-\lambda^*}}{\alpha_0} - 1\right)$ and $\beta_2(h_1) = \alpha_0/\gamma(h_1) + \eta^*\xi\tau$.

$$\begin{aligned} T_3^{\text{UB}}(h_1) &= \Bigg[e^{-\beta_3(h_1) - \frac{\alpha_0}{\omega_{\lambda^*}}} - e^{-\psi(h_1) + \alpha_0 - \beta_3(h_1)} \\ &\quad - \frac{\alpha_0\eta^*\xi\tau}{\omega_{\lambda^*}^2} e^{\frac{\alpha_0\eta^*\xi\tau}{\omega_{\lambda^*}^2} - \frac{\eta^*\xi\tau}{\omega_{\lambda^*}} - \frac{\alpha_0}{\omega_{\lambda^*}}} \\ &\quad \times E_1\left(\beta_3(h_1) + \frac{\alpha_0\eta^*\xi\tau}{\omega_{\lambda^*}^2} - \frac{\eta^*\xi\tau}{\omega_{\lambda^*}}\right)\Bigg] \mathbb{1}_{\left\{\psi(h_1) - \alpha_0 > \frac{\alpha_0}{\omega_{\lambda^*}}\right\}}, \end{aligned} \quad (34)$$

where $\beta_3(h_1) = \eta^*\xi\tau/(\omega_{\lambda^*} - \alpha_0/\left[\psi(h_1) - \alpha_0\right])$.

Proof: The proof is given in Appendix H. ∎

The expectation over h_1 in (30) can be computed efficiently using Gauss-Laguerre quadrature [31, Ch. 25.4] as follows:

$$\begin{aligned} P_{\text{out}}^{\text{UB}}(\lambda^*) \approx N_t e^{-\frac{\alpha_0}{\omega_{\lambda^*}}} \sum_{m=1}^{\mathsf{GL}} w_m e^{-\frac{\eta^*\xi\tau}{\omega_{\lambda^*} - \frac{\alpha_0}{x_m + \alpha_0/\omega_{\lambda^*}}}} \\ \times \left[T_0\left(x_m + \frac{\alpha_0}{\omega_{\lambda^*}})\right) + T_1^{\text{UB}}\left(x_m + \frac{\alpha_0}{\omega_{\lambda^*}}\right) \right. \\ \left. + T_2^{\text{UB}}\left(x_m + \frac{\alpha_0}{\omega_{\lambda^*}}\right) + T_3^{\text{UB}}\left(x_m + \frac{\alpha_0}{\omega_{\lambda^*}}\right)\right]^{N_t-1}, \end{aligned} \quad (35)$$

where x_m and w_m, for $1 \le m \le \mathsf{GL}$, are the abscissas and weights, respectively [31, Table 25.9], and GL is the number of terms.

V. Benchmarking and Numerical Results

We benchmark the EE, average rate, and average power consumption of EE-ASPA with several rules considered in the literature, namely, minimum interference rule [21], maximum ratio rule [22], and maximum received signal power rule [20]. We also compare with the rate-optimal rule in (18). We do not compare with the schemes in [12]–[14], [16] because their system models are inherently different. The performance metrics for all the rules are obtained from Monte Carlo simulations that average over $10,000$ fade realizations. The path-losses of the STx-SRx link (μ_h) and STx-PRx link (μ_g) are -114 dB and -121 dB, respectively, bandwidth is 1 MHz, $\sigma_n^2 = -113.8$ dBm, $P_c = 98$ mW, and $\xi = 2.86$ [29]. In the average interference power model, $\sigma_p^2 = -106.8$ dBm. In the instantaneous interference power model, σ_p^2 is an exponential RV with mean -106.8 dBm. Unless mentioned otherwise, we employ the subgradient-based algorithm (cf. Section IV-A) to compute EE-ASPA's parameters.

The minimum interference rule selects the antenna $s = \text{argmin}_{i\in\{1,\ldots,N_t\}}\{g_i\}$. The maximum received signal power rule selects $s = \text{argmax}_{i\in\{1,\ldots,N_t\}}\{h_i P_i\}$. The maximum ratio rule selects $s = \text{argmax}_{i\in\{1,\ldots,N_t\}}\{h_i/g_i\}$. As originally proposed, these rules set the power as $P_i = \min\{P_{\max}, \tau/g_i\}$, due to which they have a zero interference-outage probability. To enable them to exploit the non-zero outage probability $O_{\max}$ and thereby ensure a fair comparison, we modify the power adaptation for these rules as follows: $P_i = P_{\max}$, if $P_{\max} \le \tau/g_i$; else,

$$P_i = \begin{cases} P_{\max}, & \text{with probability } q, \\ \dfrac{\tau}{g_i}, & \text{with probability } 1 - q, \end{cases} \quad (36)$$

where q is set numerically such that $\Pr(P_s g_s > \tau) = O_{\max}$.

Figure 4 benchmarks the EE in Mbits/J (cf. (1)) of the above rules as a function of the peak fading-averaged SINR $\bar{\Gamma} \triangleq P_{\max}\mu_h/(\sigma_n^2 + \mathbb{E}\left[P_p|\alpha_p|^2\right])$. It shows results for the two primary interference models. In both models, the EE of EE-ASPA increases as $\bar{\Gamma}$ increases and then saturates. The EE of EE-ASPA is greater than or equal to that of all the other rules, which validates its optimality that was proved in Section III. Also plotted is the EE of UC-ASPA (cf. (6)),

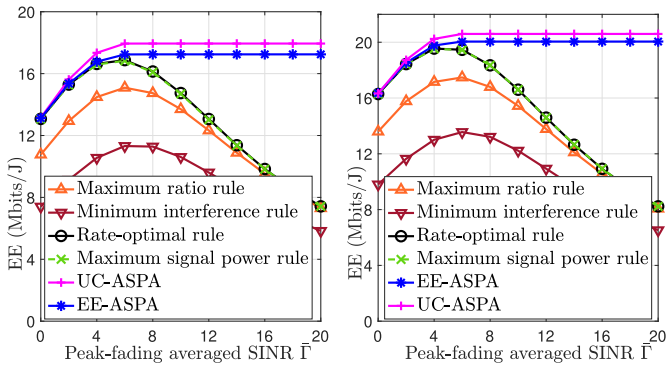

(a) Average interference power model (b) Instantaneous interference power model

Fig. 4. Benchmarking of EE of various ASPA rules as a function of $\bar{\Gamma}$ ($\tau/\sigma^2 = -3$ dB, $N_t = 4$, and $O_{\max} = 0.01$).

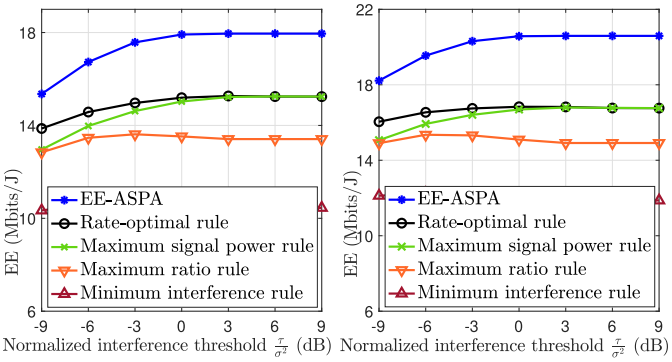

(a) Average interference power model (b) Instantaneous interference power model

Fig. 5. EE benchmarking of various ASPA rules as a function of $\frac{\tau}{\sigma^2}$ ($N_t = 4$, $O_{\max} = 0.1$, and $\bar{\Gamma} = 10$ dB).

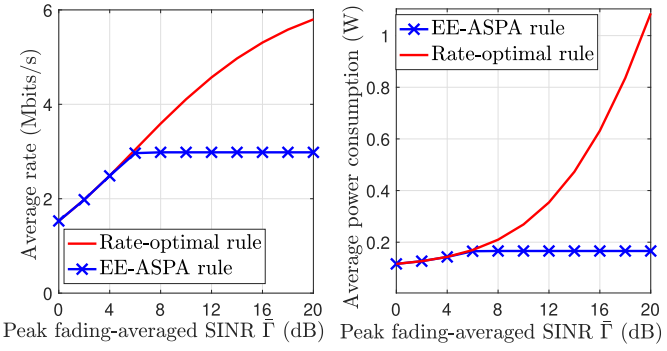

(a) Average rate (b) Average power consumption

Fig. 6. Trade-off between the average rate and the average power consumption ($N_t = 4$, $\tau/\sigma^2 = 3$ dB, and $O_{\max} = 0.05$).

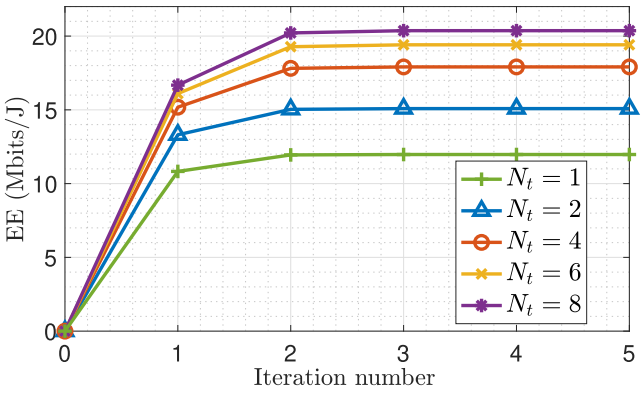

Fig. 7. Convergence of power penalty iteration and impact of number of transmit antennas ($\tau/\sigma^2 = 0$ dB, $\bar{\Gamma} = 10$ dB, and $O_{\max} = 0.1$).

which maximizes the same objective function as EE-ASPA, but ignores the interference constraint and is infeasible. The gap between the EE of EE-ASPA and UC-ASPA highlights the impact of the interference-outage constraint. For small $P_{\max}$, the peak power constraint limits the EE. Increasing $P_{\max}$, therefore, leads to an increase in the EE. However, for large $P_{\max}$, the interference-outage constraint limits the EE, which then saturates. This is unlike the other ASPA rules whose EE decreases for large $P_{\max}$. The rate-optimal rule has the same EE as EE-ASPA for $\bar{\Gamma}$ up to 4 dB. This is because, for small $P_{\max}$, the average power consumption is dominated by the constant P_c. This makes the EE and rate maximization problems equivalent.

Figure 5 benchmarks the EE as a function of τ/σ^2 for the two interference models. In both models, the EE of all rules increases as τ/σ^2 increases and then saturates. This is because the interference-outage constraint becomes looser as τ increases, and the peak power constraint eventually controls the EE. EE-ASPA achieves a higher EE than the other rules. The minimum interference rule has the lowest EE because it does not exploit the transmit diversity due to TAS for improving the secondary system's performance. In Figures 4 and 5, the trends for the two models are qualitatively similar except that the EE is lower for the average interference power model. We focus on the average interference power model henceforth.

To better understand the trade-off between rate and power consumed, Figure 6(a) compares the average rates of EE-ASPA and the rate-optimal rule, and Figure 6(b) compares the average power consumed by the two rules as a function of $\bar{\Gamma}$. For EE-ASPA, its average rate and average power consumption both increase as $\bar{\Gamma}$ increases, but they eventually saturate. On the other hand, as $\bar{\Gamma}$ increases, the average rate and average power consumption of the rate-optimal rule both keep increasing. When $\bar{\Gamma}$ is plotted in dB scale, the average rate increases linearly and the average power consumption increases exponentially for the rate-optimal rule. Thus, the EE of the rate-optimal rule eventually decreases.

Figure 7 plots the EE of EE-ASPA as a function of the number of iterations for determining η. It also studies the effect of N_t on the EE. Here, λ is found using the subgradient algorithm. We see that for any N_t, the EE increases as the number of iterations increases, as proved in Lemma 3. Notably, the algorithm converges within only three iterations. The optimal EE increases as N_t increases. For example, the EE increases by 26% and 19% when N_t increases from 1 to 2 and from 2 to 4, respectively. This shows the ability of TAS

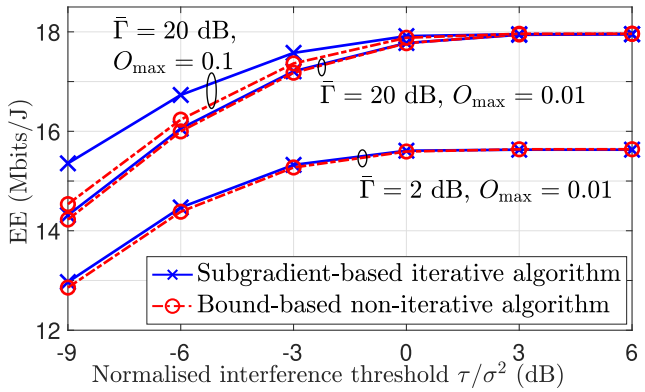

Fig. 8. EE achieved by the subgradient-based and bound-based algorithms ($N_t = 4$).

to exploit spatial diversity in underlay spectrum sharing using only one RF chain.

Figure 8 compares the subgradient-based iterative and the bound-based non-iterative algorithms. It plots the EE as a function of τ/σ^2 for three pairs of values of $O_{\max}$ and $\bar{\Gamma}$. As $O_{\max}$ increases, the EE increases because the interference-outage constraint becomes looser. The bound-based algorithm is close to the subgradient-based algorithm, i.e., it is near-optimal, for $O_{\max} = 0.01$ for all τ/σ^2 and $\bar{\Gamma}$. However, for $O_{\max} = 0.1$, it has a lower EE for smaller values of τ/σ^2 since the upper bound $P_{\text{out}}^{\text{UB}}(.)$ is less tight. For large values of τ/σ^2, the curves saturate to a value that depends on $\bar{\Gamma}$ but not $O_{\max}$. This is because, as τ increases, $\lambda \to 0$ and the peak power constraint drives the EE.

VI. Conclusion

We proposed a novel and optimal rule called EE-ASPA that maximized the EE of an underlay spectrum sharing system subject to the stochastic interference-outage and the peak power constraints. EE-ASPA was parameterized by the penalties η^* and λ^*. To determine the penalties, we proposed two algorithms, namely, the subgradient-based algorithm and the bound-based algorithm. While the former used an iterative subgradient approach, the latter employed a lower-complexity, non-iterative approach. In both cases η^*, which was also the optimal EE, was determined using very few iterations. The bound-based algorithm's EE was near-optimal for smaller values of the interference-outage probability. The explicit characterization of the optimal rule showed that the optimal power depended on which of the four regions the selected antenna's STx-SRx and STx-PRx channel gains lay in. We also saw that in the small peak power regime, the simpler binary power adaptation was optimal. EE-ASPA achieved a higher EE than several ASPA rules proposed in the literature. An interesting avenue for future work is characterizing the optimal rule for models in which the STx has only partial or statistical CSI about the STx-PRx links.

Appendix

A. Proof of Lemma 1

Consider any ASPA rule $(s, P_s) = \phi(\mathbf{h}, \mathbf{g})$ that is feasible, i.e., it satisfies the constraints in (3), (4), and (5). From the definition of ϕ^* in (7), it follows that $\Omega_{s^*}(P_{s^*}^*; \eta, \lambda) \geq \Omega_s(P_s; \eta, \lambda)$. Averaging the above inequality over $\mathbf{h}$ and $\mathbf{g}$, and rearranging terms that constitute $\Omega_i(P_i; \eta, \lambda)$ yields

$$\mathbb{E}\left[\log\left(1 + \frac{P_{s^*}^* h_{s^*}}{\sigma^2}\right) - \eta\xi P_{s^*}^*\right] \geq \mathbb{E}\left[\log\left(1 + \frac{P_s h_s}{\sigma^2}\right)\right] - \eta\xi\mathbb{E}[P_s] - \lambda\left(\mathbb{E}\left[\mathbb{1}_{\{P_s g_s > \tau\}}\right] - \mathbb{E}\left[\mathbb{1}_{\{P_{s^*}^* g_{s^*} > \tau\}}\right]\right). \quad (37)$$

We know that $\mathbb{E}\left[\mathbb{1}_{\{P_s g_s > \tau\}}\right] = \Pr(P_s g_s > \tau) \leq O_{\max}$ since ϕ is a feasible ASPA rule. Furthermore, from the choice of λ, we have $\mathbb{E}\left[\mathbb{1}_{\{P_{s^*}^* g_{s^*} > \tau\}}\right] = O_{\max}$. Therefore,

$$\mathbb{E}\left[\mathbb{1}_{\{P_s g_s > \tau\}}\right] - \mathbb{E}\left[\mathbb{1}_{\{P_{s^*}^* g_{s^*} > \tau\}}\right] = \Pr(P_s g_s > \tau) - O_{\max} \leq 0. \quad (38)$$

Hence, $\mathbb{E}\left[\log\left(1 + \frac{P_{s^*}^* h_{s^*}}{\sigma^2}\right) - \eta\xi P_{s^*}^*\right] \geq \mathbb{E}\left[\log\left(1 + \frac{P_s h_s}{\sigma^2}\right) - \eta\xi P_s\right]$. Thus, EE-ASPA solves $\mathcal{P}_1(\eta)$.

B. Proof of Lemma 2

We are given that the maximum value of the objective function of $\mathcal{P}_1(\eta^*)$ is 0. We also know from Lemma 1 that ϕ^* in (7) maximizes the objective function of $\mathcal{P}_1(\eta^*)$ when $\eta = \eta^*$. Let $(s, P_s) = \phi(\mathbf{h}, \mathbf{g})$ be any feasible ASPA rule. Hence,

$$\mathbb{E}\left[\log\left(1 + \frac{P_s h_s}{\sigma^2}\right)\right] - \eta^*\mathbb{E}[\xi P_s + P_c] \leq 0, \quad \text{for any feasible rule } \phi, \quad (39a)$$

$$\mathbb{E}\left[\log\left(1 + \frac{P_{s^*}^* h_{s^*}}{\sigma^2}\right)\right] - \eta^*\mathbb{E}[\xi P_{s^*}^* + P_c] = 0, \quad \text{for the rule } \phi^*. \quad (39b)$$

Upon rearranging terms, we get $\eta^* = \frac{\mathbb{E}\left[\log\left(1+\frac{P_{s^*}^* h_{s^*}}{\sigma^2}\right)\right]}{\mathbb{E}\left[\xi P_{s^*}^* + P_c\right]} \geq \frac{\mathbb{E}\left[\log\left(1+\frac{P_s h_s}{\sigma^2}\right)\right]}{\mathbb{E}[\xi P_s + P_c]}$. Hence, the result follows.[3]

C. Brief Proof of Lemma 3

Define the function $Q(\eta) = \max_{\phi \in \widetilde{\mathcal{D}}} \left\{\mathbb{E}\left[\log\left(1 + \frac{P_s h_s}{\sigma^2}\right)\right] - \eta\mathbb{E}[\xi P_s + P_c]\right\}$, where $\widetilde{\mathcal{D}} \subset \mathcal{D}$ is the set of all feasible rules. Using an approach similar to [33], we can show the following:

(a) $Q(\eta)$ is a strictly monotonically decreasing function of η.

(b) $Q(\hat{\eta}) \geq 0$ for any $\hat{\phi}(.) = \left(\hat{s}, \hat{P}_{\hat{s}}\right) \in \widetilde{\mathcal{D}}$ such that

$$\hat{\eta} = \frac{\mathbb{E}\left[\log\left(1 + \frac{\hat{P}_{\hat{s}} h_{\hat{s}}}{\sigma^2}\right)\right]}{\mathbb{E}\left[\xi \hat{P}_{\hat{s}} + P_c\right]}.$$

From (10), in the u^{th} iteration, for $u \geq 0$, we get

$$\mathbb{E}\left[\log\left(1 + \frac{P_{s^{(u)}} h_{s^{(u)}}}{\sigma^2}\right)\right] = \eta^{(u+1)}\mathbb{E}[\xi P_{s^{(u)}} + P_c]. \quad (40)$$

[3]The proof uses ideas from [33]. However, our problem is a stochastic fractional programming problem in which the numerator and denominator of the objective function in (2) are both expectations, while this is not so in [33].

From the definition of $Q(\eta)$, we get $Q\left(\eta^{(u)}\right) = \mathbb{E}\left[\log\left(1+\frac{P_{s^{(u)}}h_{s^{(u)}}}{\sigma^2}\right)\right] - \eta^{(u)}\mathbb{E}\left[\xi P_{s^{(u)}}+P_c\right]$. Substituting (40) in this equation and applying the property in (b) yields $\eta^{(u+1)} \geq \eta^{(u)}$ for all u with $Q\left(\eta^{(u)}\right) \geq 0$.

Since the sequence $\eta^{(0)}, \eta^{(1)}, \ldots$ is strictly monotonically increasing and bounded, it converges. Suppose it converges to $\bar{\eta} < \eta^*$. By the construction of the EE-ASPA algorithm, from Section III-B, we get $Q(\bar{\eta}) = 0$. And, from Lemma 2, we know that $Q(\eta^*) = 0$. This contradicts the strict monotonic property of $Q(\eta)$ in (a). Hence, the sequence $\left\{\eta^{(u)}\right\}$ must converge to η^*.

D. Proof of Result 1

The reward function in (8) takes the following forms depending on the values of P_i and τ/g_i:

$$\Omega_i(P_i;\eta^*,\lambda^*) = \begin{cases} \log\left(1+\frac{P_i h_i}{\sigma^2}\right) - \eta^*\xi P_i, \text{ for } P_i \leq \frac{\tau}{g_i}, & \text{(41a)} \\ \log\left(1+\frac{P_i h_i}{\sigma^2}\right) - \eta^*\xi P_i - \lambda^*, \text{ for } P_i > \frac{\tau}{g_i}. & \text{(41b)} \end{cases}$$

We consider the two cases $P_{\max} \leq \tau/g_i$ and $P_{\max} > \tau/g_i$ separately below.

1) $P_{\max} \leq \tau/g_i$*:* This corresponds to the region $\mathcal{R}_1$ in (12a). For this case, $P_i \leq \tau/g_i$ since $P_i \leq P_{\max}$. Thus, the reward function simplifies to (41a), which is a concave function of P_i. From the first order conditions, we can show that $\widetilde{P}(h_i)$ in (15) maximizes $\Omega_i(P_i;\eta^*,\lambda^*)$. Accounting for the peak power constraint, we get $P_i^* = \min\left\{\widetilde{P}(h_i), P_{\max}\right\}$.
2) $P_{\max} > \tau/g_i$*:* In this case, the following three subcases arise depending on where $\widetilde{P}(h_i)$ lies with respect to τ/g_i and $P_{\max}$:
   a) $\widetilde{P}(h_i) \leq \tau/g_i < P_{\max}$*:* Rearranging the terms in $\widetilde{P}(h_i) \leq \tau/g_i$ and the expression for $\widetilde{P}(h_i)$ in (15), we get $h_i \leq \alpha_1(g_i)$, where $\alpha_1(g_i)$ is given in (13). This corresponds to the region $\mathcal{R}_2$ in (12b). The reward function is given by (41a) for $P_i \in (0, \tau/g_i]$, and by (41b) otherwise. Since $\widetilde{P}(h_i) \leq \tau/g_i$, it follows from the above discussion that it maximizes $\Omega_i(P_i;\eta^*,\lambda^*)$. Also, $\widetilde{P}(h_i) < P_{\max}$ in $\mathcal{R}_2$. Therefore, $P_i^* = \widetilde{P}(h_i)$. This yields (14b).
   b) $\tau/g_i < \widetilde{P}(h_i) \leq P_{\max}$*:* From (15), we can show that this condition is equivalent to $\alpha_1(g_i) < h_i \leq \alpha_2$, where α_2 is given in (13). This corresponds to the region $\mathcal{R}_3$ in (12c). Since $\widetilde{P}(h_i) > \tau/g_i$, $\Omega_i(P_i;\eta^*,\lambda^*)$ in (41a) is a monotonically increasing function for $P_i \in [0, \tau/g_i]$. Thereafter, it decreases by λ^* at $P_i = \tau/g_i$. It is monotonically increasing for $P_i \in (\tau/g_i, \widetilde{P}(h_i)]$, and is monotonically decreasing for $P_i \in (\widetilde{P}(h_i), P_{\max}]$. Hence, the reward function is maximized at either τ/g_i or $\widetilde{P}(h_i)$. This leads to (14c).
   c) $\tau/g_i < P_{\max} < \widetilde{P}(h_i)$*:* This is equivalent to $h_i > \alpha_2$. This corresponds to the region $\mathcal{R}_4$ in (12d). Since $\widetilde{P}(h_i) > P_{\max}$, it cannot be the optimal power. $\Omega_i(P_i;\eta^*,\lambda^*)$ is monotonically increasing in $P_i \in [0, \tau/g_i]$. It decreases by λ^* at $P_i = \tau/g_i$. It again monotonically increases in $P_i \in (\tau/g_i, P_{\max}]$. Hence, P_i^* is either τ/g_i or $P_{\max}$.

Substituting the optimal power in (7) yields the optimal antenna in (11).

E. Brief Proof of Corollary 2

As in Appendix D, we consider the cases $P_{\max} \leq \tau/g_i$ and $P_{\max} > \tau/g_i$ separately.

1) $P_{\max} \leq \tau/g_i$*:* In this case, $(h_i, g_i) \in \mathcal{R}_1$. Therefore, $P_i^* = \widetilde{P}(h_i) \leq P_{\max}$ for $0 \leq h_i \leq \alpha_2$. From (15), $\widetilde{P}(h_i)$ is a non-decreasing function of h_i. And, $P_i^* = P_{\max}$ for $h_i > \alpha_2$.
2) $P_{\max} > \tau/g_i$*:* We have $(h_i, g_i) \in \mathcal{R}_2$ for $h_i \in [0, \alpha_1(g_i)]$. It follows from (14b) that $P_i^* = \widetilde{P}(h_i)$. It is a non-decreasing function of h_i. It equals τ/g_i at $h_i = \alpha_1(g_i)$.
   a) *When* $\alpha_3(g_i) \leq \alpha_2$*:* In the interval $(\alpha_1(g_i), \alpha_2]$, $(h_i, g_i) \in \mathcal{R}_3$. From (14c) and from the definition of $\alpha_3(g_i)$ in (16), it follows that $P_i^* = \tau/g_i$ for $h_i \in (\alpha_1(g_i), \alpha_3(g_i)]$, and $P_i^* = \widetilde{P}(h_i) > \tau/g_i$ for $h_i \in (\alpha_3(g_i), \alpha_2]$. Thus, P_i^* is constant for $h_i \in (\alpha_1(g_i), \alpha_3(g_i)]$, it jumps to a higher value at $h_i = \alpha_3(g_i)$, and monotonically increases in $h_i \in (\alpha_3(g_i), \alpha_2]$. It equals $P_{\max}$ at $h_i = \alpha_2$. For $h_i \in (\alpha_2, \infty)$, it is in $\mathcal{R}_4$. From above, it follows that $\Omega_i(P_{\max};\eta^*,\lambda^*) \geq \Omega_i(\tau/g_i;\eta^*,\lambda^*)$ at $h_i = \alpha_2$. Also, we can show that $\frac{\partial\Omega_i(P_{\max};\eta^*,\lambda^*)}{\partial h_i} > \frac{\partial\Omega_i(\tau/g_i;\eta^*,\lambda^*)}{\partial h_i}$ for $P_{\max} > \tau/g_i$. Hence, $\Omega_i(P_{\max};\eta^*,\lambda^*) > \Omega_i(\tau/g_i;\eta^*,\lambda^*)$ for $h_i \in (\alpha_2, \infty)$. Thus, P_i^* remains at $P_{\max}$ for $h_i \in (\alpha_2, \infty)$.
   b) *When* $\alpha_3(g_i) > \alpha_2$*:* Along lines similar to the above cases, we can prove that $P_i^* = \tau/g_i$ is constant for $h_i \in (\alpha_1(g_i), \widetilde{\alpha}_3(g_i)]$, jumps and increases to $P_{\max}$ at $h_i = \widetilde{\alpha}_3(g_i)$, and remains there. We skip the details to conserve space

Thus, P_i^* is a monotonically non-decreasing function of h_i in all cases.

F. Brief Proof of Result 2

From (20), an interference-outage occurs if and only if $h_{s^*} > \alpha_0$ and $P_{\max} g_{s^*} > \tau$. Hence, by the law of total probability and symmetry, we have $P_{\text{out}} = N_t \Pr\left(s^*=1, g_1 > \frac{\tau}{P_{\max}}, h_1 > \alpha_0\right)$. Since the channel power gains are independent, this can be further simplified as

$$P_{\text{out}} = N_t \Pr\left(h_1 > h_2, \ldots, h_1 > h_{N_t}, h_1 > \alpha_0, g_1 > \frac{\tau}{P_{\max}}\right). \quad (42)$$

Conditioning and averaging over h_1 yields (21).

From (20), for Rayleigh fading, it follows that $f_{h_{s^*}}(x) = N_t e^{-x}\left(1-e^{-x}\right)^{N_t-1}$ for $x \geq 0$. Expanding $\left(1-e^{-x}\right)^{N_t-1}$ and simplifying, we can show that the average rate equals

$$\begin{aligned}\mathbb{E}\left[\log\left(1+\frac{P_{s^*}^* h_{s^*}}{\sigma^2}\right)\right] &= N_t \sum_{m=0}^{N_t-1}\binom{N_t-1}{m}\frac{(-1)^m}{m+1} \\ &\times\left[\log\left(1+\frac{\alpha_0 P_{\max}}{\sigma^2}\right)e^{-(m+1)\alpha_0}\right. \\ &\left.+e^{\frac{(m+1)\sigma^2}{P_{\max}}}E_1\left((m+1)\left[\frac{\sigma^2}{P_{\max}}+\alpha_0\right]\right)\right]. \quad (43)\end{aligned}$$

Similarly, the average power consumed equals $\mathbb{E}\left[\xi P_{s^*}^* + P_c\right] = P_{\max}\xi\left[1-\left(1-e^{-\alpha_0}\right)^{N_t}\right] + P_c$. Taking the ratio of (43) and the above equation yields (22).

G. Proof of Lemma 4

For antenna i, let $R_y^z(i)$ denote the event that $(h_i, g_i) \in \mathcal{R}_y^z$, where $y \in \{2,3\}$ and $z \in \{\text{ZP, NOI, TP, OI}\}$. From Section III-F, an interference-outage occurs only when $(h_{s^*}, g_{s^*}) \in \mathcal{R}_3^{\text{OI}}$. Hence, by symmetry and the law of total probability, we get

$$P_{\text{out}} = \Pr\left(R_3^{\text{OI}}(s^*)\right) = N_t \Pr\left(s^*=1, R_3^{\text{OI}}(1)\right). \quad (44)$$

Consider the remaining antennas $2,3,\ldots,N_t$. Let j, k, l, and n be the number of antennas that lie in the regions $\mathcal{R}_2^{\text{ZP}}, \mathcal{R}_2^{\text{NOI}}, \mathcal{R}_3^{\text{TP}}$, and $\mathcal{R}_3^{\text{OI}}$, respectively. Let one such event F_{jkln} be

$$\begin{aligned}F_{jkln} = \{&R_2^{\text{ZP}}(2),\ldots,R_2^{\text{ZP}}(j+1), R_2^{\text{NOI}}(j+2),\ldots, \\ &R_2^{\text{NOI}}(j+k+1), R_3^{\text{TP}}(j+k+2),\ldots, \\ &R_3^{\text{TP}}(j+k+l+1), \\ &R_3^{\text{OI}}(j+k+l+2),\ldots,R_3^{\text{OI}}(N_t)\}. \quad (45)\end{aligned}$$

By the law of total probability and symmetry, we get

$$\begin{aligned}&\Pr\left(s^*=1, R_3^{\text{OI}}(1)\right) \\ &= \sum_{\substack{j,k,l,n\geq 0,\\ j+k+l+n=N_t-1}} \frac{(N_t-1)!}{j!k!l!n!}\Pr\left(s^*=1, R_3^{\text{OI}}(1), F_{jkln}\right). \end{aligned} \quad (46)$$

From (11), antenna 1 is selected if $\Omega_1\left(P_1^*;\eta^*,\lambda^*\right) > \Omega_i\left(P_i^*;\eta^*,\lambda^*\right)$, for all $i \in \{2,\ldots,N_t\}$. Substituting this and (45) in (46), we get

$$\begin{aligned}&\Pr\left(s^*=1, R_3^{\text{OI}}(1), F_{jkln}\right) \\ &= \Pr\Big[\Omega_1\left(\widetilde{P}\left(h_1\right);\eta^*,\lambda^*\right) > \Omega_2\left(0;\eta^*,\lambda^*\right),\ldots, \\ &\quad \Omega_1\left(\widetilde{P}\left(h_1\right);\eta^*,\lambda^*\right) > \Omega_{N_t}\left(\widetilde{P}\left(h_{N_t}\right);\eta^*,\lambda^*\right), \\ &\quad R_3^{\text{OI}}(1), R_2^{\text{ZP}}(2),\ldots,R_2^{\text{ZP}}(j+1), \\ &\quad R_2^{\text{NOI}}(j+2),\ldots,R_2^{\text{NOI}}(j+k+1), R_3^{\text{TP}}(j+k+2), \\ &\quad \ldots, R_3^{\text{TP}}(j+k+l+1), R_3^{\text{OI}}(j+k+l+2), \\ &\quad \ldots, R_3^{\text{OI}}(N_t)\Big]. \quad (47)\end{aligned}$$

Conditioning on h_1 and then taking expectation over it, we get the following by symmetry:

$$\begin{aligned}&\Pr\left(s^*=1, R_3^{\text{OI}}(1), F_{jkln}\right) \\ &= \mathbb{E}\Big[\Pr\left(R_3^{\text{OI}}(1) \mid h_1\right) \\ &\quad\times\left[\Pr\left(R_2^{\text{ZP}}(2), \Omega_1\left(\widetilde{P}\left(h_1\right);\eta^*,\lambda^*\right) > 0 \mid h_1\right)\right]^j \\ &\quad\times\Big[\Pr\Big(R_2^{\text{NOI}}(2), \Omega_1\left(\widetilde{P}\left(h_1\right);\eta^*,\lambda^*\right) \\ &\qquad > \Omega_2\left(\widetilde{P}\left(h_2\right);\eta^*,\lambda^*\right) \mid h_1\Big)\Big]^k \\ &\quad\times\Big[\Pr\Big(R_3^{\text{TP}}(2), \Omega_1\left(\widetilde{P}\left(h_1\right);\eta^*,\lambda^*\right) \\ &\qquad > \Omega_2\left(\frac{\tau}{g_2};\eta^*,\lambda^*\right) \mid h_1\Big)\Big]^l \\ &\quad\times\Big[\Pr\Big(R_3^{\text{OI}}(2), \Omega_1\left(\widetilde{P}\left(h_1\right);\eta^*,\lambda^*\right) \\ &\qquad > \Omega_2\left(\widetilde{P}\left(h_2\right);\eta^*,\lambda^*\right) \mid h_1\Big)\Big]^n\Big]. \quad (48)\end{aligned}$$

Substituting (48) in (46) and then in the expression for P_{out} in (44) and simplifying yields (25).

H. Brief Proof of Result 3

We derive exact expressions or upper bounds for each term in (25).

1) Pr $(h_1 > \alpha_3(g_1) \mid h_1)$: By the law of total probability, we get

$$\begin{aligned}\Pr\left(h_1 > \alpha_3(g_1) \mid h_1\right) &= \Pr\left(h_1 > \alpha_3(g_1), g_1 > \frac{\eta^*\xi\tau}{\omega_{\lambda^*}} \mid h_1\right) \\ &+\Pr\left(h_1 > \alpha_3(g_1), g_1 \leq \frac{\eta^*\xi\tau}{\omega_{\lambda^*}} \mid h_1\right).\end{aligned}$$

Substituting the expression for $\alpha_3(g_i)$ from (16) and rearranging, we get

$$\begin{aligned}&\Pr\left(h_1 > \alpha_3(g_1) \mid h_1\right) \\ &= \Pr\left(g_1 > \frac{\eta^*\xi\tau}{\omega_{\lambda^*}-\frac{\alpha_0}{h_1}} \mid h_1\right)\mathbb{1}_{\left\{h_1 > \frac{\alpha_0}{\omega_{\lambda^*}}\right\}}, \\ &= e^{-\eta^*\xi\tau/\left(\omega_{\lambda^*}-\frac{\alpha_0}{h_1}\right)}\mathbb{1}_{\left\{h_1 > \frac{\alpha_0}{\omega_{\lambda^*}}\right\}}. \end{aligned} \quad (49)$$

2) $T_0(h_1)$: When $(h_1, g_1) \in \mathcal{R}_3^{\text{OI}}$, substituting (15) in (8) and using $\alpha_0 = \eta^*\xi\sigma^2$ yields $\Omega_1\left(\widetilde{P}\left(h_1\right);\eta^*,\lambda^*\right) = \log\left(\frac{h_1}{\alpha_0}\right) - 1 + \frac{\alpha_0}{h_1} - \lambda^*$. Substituting this in the expression for $T_0(h_1)$ in (26) and rearranging terms, we get

$$\begin{aligned}T_0(h_1) &= \Pr\left(\psi(h_1) > \alpha_0\, e^{1+\lambda^*}, h_2 \leq \alpha_0 \mid h_1\right), \\ &= \left(1-e^{-\alpha_0}\right)\mathbb{1}_{\left\{\psi(h_1) > \alpha_0 e^{1+\lambda^*}\right\}}, \end{aligned} \quad (50)$$

where $\psi(h_1) = h_1 e^{\frac{\alpha_0}{h_1}}$.

3) Upper Bound for $T_1(h_1)$: When $(h_2, g_2) \in \mathcal{R}_2^{\text{NOI}}$, as in the above case, we can show that $\Omega_2\left(\widetilde{P}\left(h_2\right);\eta^*,\lambda^*\right) = \log\left(\frac{h_2}{\alpha_0}\right) - 1 + \frac{\alpha_0}{h_2}$. Substituting this and the above expression

for $\Omega_1\left(\widetilde{P}\,(h_1);\eta^*,\lambda^*\right)$ in (27), applying $h_2 e^{\frac{\alpha_0}{h_2}} \geq h_2+\alpha_0$, and simplifying, we get

$$T_1(h_1) \leq \Pr\left(\alpha_0 < h_2 \leq \min\left\{\psi(h_1)e^{-\lambda^*}-\alpha_0, \alpha_1(g_2)\right\} \mid h_1\right). \tag{51}$$

To simplify this further, we condition and average over g_2. This yields

$$T_1(h_1) \leq \mathbb{1}_{\left\{\psi(h_1)e^{-\lambda^*}>2\alpha_0\right\}} \times\left(e^{-\alpha_0} - \mathbb{E}\left[e^{-\min\left\{\psi(h_1)e^{-\lambda^*}-\alpha_0,\alpha_1(g_2)\right\}} \mid g_2, h_1\right]\right). \tag{52}$$

Let $\psi(h_1)e^{-\lambda^*}-\alpha_0=\alpha_1(g_2)$ at $g_2=\beta_1(h_1)$. From (13), we get $\beta_1(h_1)=\eta^*\xi\tau/\left(1-\alpha_0/\left[\psi(h_1)e^{-\lambda^*}-\alpha_0\right]\right)$. It is easy to verify that for $g_2<\beta_1(h_1)$, we have $\psi(h_1)e^{-\lambda^*}-\alpha_0<\alpha_1(g_2)$, and for $g_2\geq\beta_1(h_1)$, we have $\psi(h_1)e^{-\lambda^*}-\alpha_0\geq\alpha_1(g_2)$. Thus, (52) simplifies to

$$T_1(h_1) \leq \left[e^{-\alpha_0} - e^{\alpha_0-\psi(h_1)e^{-\lambda^*}}\left(1-e^{-\beta_1(h_1)}\right) - e^{-\alpha_0}\int_{\beta_1(h_1)}^{\infty} e^{\frac{-\alpha_0\eta^*\xi\tau}{g_2-\eta^*\xi\tau}}\, e^{-g_2}\, dg_2\right]\mathbb{1}_{\left\{\psi(h_1)e^{-\lambda^*}>2\alpha_0\right\}}. \tag{53}$$

Since $e^{\frac{-\alpha_0\eta^*\xi\tau}{g_2-\eta^*\xi\tau}}$ increases monotonically in $(\eta^*\xi\tau,\infty)$, it follows that $e^{\frac{-\alpha_0\eta^*\xi\tau}{g_2-\eta^*\xi\tau}} \geq e^{\frac{-\alpha_0\eta^*\xi\tau}{\beta_1(h_1)-\eta^*\xi\tau}}$ for $g_2\geq\beta_1(h_1)$. Applying this in (53) and integrating yields the upper bound for $T_1(h_1)$ in (32).

4) Upper Bounds for $T_2(h_1)$ and $T_3(h_1)$: These are derived using techniques similar to those used above. We skip the details due to space constraints.

REFERENCES

[1] S. Naduvilpattu and N. B. Mehta, "Optimal energy-efficient antenna selection and power adaptation for underlay spectrum sharing," in *Proc. IEEE Int. Conf. Commun. (ICC)*, Jun. 2021, pp. 1–6.

[2] Z. Zhang *et al.*, "6G wireless networks: Vision, requirements, architecture, and key technologies," *IEEE Veh. Technol. Mag.*, vol. 14, no. 3, pp. 28–41, Sep. 2019.

[3] Y. Cao *et al.*, "Optimization or alignment: Secure primary transmission assisted by secondary networks," *IEEE J. Sel. Areas Commun.*, vol. 36, no. 4, pp. 905–917, Apr. 2018.

[4] N. B. Mehta, S. Kashyap, and A. F. Molisch, "Antenna selection in LTE: From motivation to specification," *IEEE Commun. Mag.*, vol. 50, no. 10, pp. 144–150, Oct. 2012.

[5] R. Sarvendranath and N. B. Mehta, "Exploiting power adaptation with transmit antenna selection for interference-outage constrained underlay spectrum sharing," *IEEE Trans. Commun.*, vol. 68, no. 1, pp. 480–492, Jan. 2020.

[6] R. Sarvendranath and N. B. Mehta, "Antenna selection with power adaptation in interference-constrained cognitive radios," *IEEE Trans. Commun.*, vol. 62, no. 3, pp. 786–796, Mar. 2014.

[7] M. Hanif, H.-C. Yang, and M.-S. Alouini, "Transmit antenna selection for power adaptive underlay cognitive radio with instantaneous interference constraint," *IEEE Trans. Commun.*, vol. 65, no. 6, pp. 2357–2367, Jun. 2017.

[8] M. F. Hanif, P. J. Smith, D. P. Taylor, and P. A. Martin, "MIMO cognitive radios with antenna selection," *IEEE Trans. Wireless Commun.*, vol. 10, no. 11, pp. 3688–3699, Nov. 2011.

[9] H. Li, J. Cheng, Z. Wang, and H. Wang, "Joint antenna selection and power allocation for an energy-efficient massive MIMO system," *IEEE Wireless Commun. Lett.*, vol. 8, no. 1, pp. 257–260, Feb. 2019.

[10] Z. Wang and L. Vandendorpe, "Antenna selection for energy efficient MISO systems," *IEEE Commun. Lett.*, vol. 21, no. 12, pp. 2758–2761, Dec. 2017.

[11] X. Zhou, B. Bai, and W. Chen, "An iterative algorithm for joint antenna selection and power adaptation in energy efficient MIMO," in *Proc. IEEE Int. Conf. Commun. (ICC)*, Jun. 2014, pp. 3812–3816.

[12] F. Zhou, N. C. Beaulieu, Z. Li, J. Si, and P. Qi, "Energy-efficient optimal power allocation for fading cognitive radio channels: Ergodic capacity, outage capacity, and minimum-rate capacity," *IEEE Trans. Wireless Commun.*, vol. 15, no. 4, pp. 2741–2755, Apr. 2016.

[13] L. Wang, M. Sheng, X. Wang, Y. Zhang, and X. Ma, "Mean energy efficiency maximization in cognitive radio channels with PU outage constraint," *IEEE Commun. Lett.*, vol. 19, no. 2, pp. 287–290, Feb. 2015.

[14] L. Sboui, Z. Rezki, and M.-S. Alouini, "Energy-efficient power allocation for underlay cognitive radio systems," *IEEE Trans. Cogn. Commun. Netw.*, vol. 1, no. 3, pp. 273–283, Sep. 2015.

[15] J. Mao, G. Xie, J. Gao, and Y. Liu, "Energy efficiency optimization for cognitive radio MIMO broadcast channels," *IEEE Commun. Lett.*, vol. 17, no. 2, pp. 337–340, Feb. 2013.

[16] M. R. Mili, L. Musavian, K. A. Hamdi, and F. Marvasti, "How to increase energy efficiency in cognitive radio networks," *IEEE Trans. Commun.*, vol. 64, no. 5, pp. 1829–1843, May 2016.

[17] L. Musavian and S. Aissa, "Fundamental capacity limits of cognitive radio in fading environments with imperfect channel information," *IEEE Trans. Commun.*, vol. 57, no. 11, pp. 3472–3480, Nov. 2009.

[18] S. Kashyap and N. B. Mehta, "Optimal binary power control for underlay CR with different interference constraints and impact of channel estimation errors," *IEEE Trans. Commun.*, vol. 62, no. 11, pp. 3753–3764, Nov. 2014.

[19] R. Sarvendranath and N. B. Mehta, "Statistical CSI driven transmit antenna selection and power adaptation in underlay spectrum sharing systems," *IEEE Trans. Commun.*, vol. 69, no. 5, pp. 2923–2934, May 2021.

[20] F. A. Khan, K. Tourki, M.-S. Alouini, and K. A. Qaraqe, "Performance analysis of a power limited spectrum sharing system with TAS/MRC," *IEEE Trans. Signal Process.*, vol. 62, no. 4, pp. 954–967, Feb. 2014.

[21] H. Y. Kong and A. Asaduzzaman, "On the outage behavior of interference temperature limited CR-MISO channel," *J. Commun. Netw.*, vol. 13, no. 5, pp. 456–462, Oct. 2011.

[22] K. Tourki, F. A. Khan, K. A. Qaraqe, H.-C. Yang, and M.-S. Alouini, "Exact performance analysis of MIMO cognitive radio systems using transmit antenna selection," *IEEE J. Sel. Areas Commun.*, vol. 32, no. 3, pp. 425–438, Mar. 2014.

[23] G. Huang and J. K. Tugnait, "On energy efficient MIMO-assisted spectrum sharing for cognitive radio networks," in *Proc. IEEE Int. Conf. Commun. (ICC)*, Jun. 2013, pp. 2644–2649.

[24] C. Jiang and L. J. Cimini, "Antenna selection for energy-efficient MIMO transmission," *IEEE Wireless Commun. Lett.*, vol. 1, no. 6, pp. 577–580, Dec. 2012.

[25] X. Wang *et al.*, "Energy efficiency optimization for NOMA-based cognitive radio with energy harvesting," *IEEE Access*, vol. 7, pp. 139172–139180, 2019.

[26] S. Jin and X. Zhang, "Optimal energy efficient scheme for MIMO-based cognitive radio networks with antenna selection," in *Proc. 49th Annu. Conf. Inf. Sci. Syst. (CISS)*, Mar. 2015, pp. 1–6.

[27] Y. Wang and J. P. Coon, "Difference antenna selection and power allocation for wireless cognitive systems," *IEEE Trans. Commun.*, vol. 59, no. 12, pp. 3494–3503, Dec. 2011.

[28] X. Kang, Y. C. Liang, A. Nallanathan, H. K. Garg, and R. Zhang, "Optimal power allocation for fading channels in cognitive radio networks: Ergodic capacity and outage capacity," *IEEE Trans. Wireless Commun.*, vol. 8, no. 2, pp. 940–950, Feb. 2009.

[29] S. Cui, A. J. Goldsmith, and A. Bahai, "Energy-efficiency of MIMO and cooperative MIMO techniques in sensor networks," *IEEE J. Sel. Areas Commun.*, vol. 22, no. 6, pp. 1089–1098, Aug. 2004.

[30] R. M. Corless, G. H. Gonnet, D. E. G. Hare, D. J. Jeffrey, and D. E. Knuth, "On the Lambert W function," *Adv. Comput. Math.*, vol. 5, pp. 329–359, Dec. 1996.

[31] M. Abramowitz and I. Stegun, *Handbook of Mathematical Functions: With Formulas, Graphs, and Mathematical Tables*. Mineola, NY, USA: Dover, 1965.

[32] D. P. Bertsekas, *Convex Optimization Algorithms*. Nashua, NH, USA: Athena Scientific, 2015.
[33] W. Dinkelbach, "On nonlinear fractional programming," *Manage. Sci.*, vol. 13, no. 7, pp. 492–498, Mar. 1967.

Suji Naduvilpattu (Student Member, IEEE) received the Bachelor of Technology degree in electronics and communication engineering from the Government College of Engineering, Kannur, Kerala, India, in 2009, and the Master of Technology degree in telecommunication from the National Institute of Technology, Calicut, Kerala, in 2012. She is currently pursuing the Ph.D. degree with the Department of Electrical Communication Engineering, Indian Institute of Science, Bengaluru. Her research interests include wireless communications, spectrum sharing, and reconfigurable intelligent surfaces.

Neelesh B. Mehta (Fellow, IEEE) received the B.Tech. degree in electronics and communications engineering from the Indian Institute of Technology (IIT), Madras, in 1996, and the M.S. and Ph.D. degrees in electrical engineering from the California Institute of Technology, Pasadena, CA, USA, in 1997 and 2001, respectively. He is currently a Professor with the Department of Electrical Communication Engineering, Indian Institute of Science, Bengaluru. He is a fellow of the Indian National Science Academy, the Indian National Academy of Engineering, and the National Academy of Sciences, India. He was a recipient of the Shanti Swarup Bhatnagar Award, the Khosla Award, the Vikram Sarabhai Research Award, and the Swarnjayanti Fellowship. From 2012 to 2015, he served on the Board of Governors for the IEEE ComSoc. He served on the Executive Editorial Committee for IEEE TRANSACTIONS ON WIRELESS COMMUNICATIONS from 2014 to 2017, and served as its Chair from 2017 to 2018. He also serves as the Chair for its Steering Committee. He has served as an Editor for the IEEE TRANSACTIONS ON COMMUNICATIONS and the IEEE WIRELESS COMMUNICATION LETTERS in the past.